



and ultimately for our mobility. Large-scale trip-level data with both temporal and spatial coverage, for example based on global positioning systems (GPS) data from mobile phones or collected from fixed traffic monitoring cameras or other sensors such as Bluetooth and/or WiFi, may enable us to better diagnose current problems and develop solutions to increased congestion-levels.

At the heart of many of these developments is the estimation of travel-time between locations. Online routing services and ride-share providers,<sup>1</sup> with millions of daily requests, make all those operational and pricing decisions based on estimates of travel time. These complex decision-making processes require, first, a good understanding of the distribution of travel time and, second, valid inference methods for various quantities of this distribution.

A *route*  $\rho$  on a transportation network  $G$  consists of an  $n$ -sequence of connected edges  $\rho = \langle e_1, e_2, \dots, e_n \rangle$  that define the order of travel. Travel time  $\mathcal{T}_\rho$  is then defined as a random variable through the partial sum

$$\mathcal{T}_\rho = \sum_{e \in \rho} d_e S_e, \quad (1)$$

where  $1/S_e$  is the average speed over the edge  $e$  of unit length  $d_e$ . The distribution of speed  $S_e$  in (1) is well-studied empirically. Travel time on each edge as well as when aggregated across trips appears to be log-normally distributed (Gao et al., 2009; Lo, 2012). Yet, the log-normal, unlike the normal, is not a stable distribution, meaning that any linear combinations of it is not necessarily log-normally distributed. It is hard to infer the distribution  $\mathcal{T}_\rho$  from the distribution of its components in (1).

Researchers have proposed different methods to estimate travel-time distribution, for example by factoring-out path uncertainty (Hunter et al., 2009; Jenelius and Koutsopoulos, 2013; Zheng and J van Zuylen, 2013; Tebaldi and West, 1998), by jointly modeling travel time and the path taken (Westgate et al., 2013; Wang et al., 2019), or by using log-normal mixtures to capture congestion patterns (Woodard et al., 2017; Guo et al., 2012).

The statistics community has shown a marked interest in developing tools for network analysis, and good references exist (Kolaczyk, 2009; Kolaczyk and Csárdi, 2014). On the other hand, there is a large amount of work to model processes on network graphs. For a survey of work in transportation see Barrat et al. (2008, ch. 11), and on dynamic epidemiological networks, see Keeling and Eames (2005). Most of this work is of a mathematical nature, and statistical work on such problems is limited with some notable exceptions (Ramsay et al., 2007; Snijders et al., 2017; Burk et al., 2007; Britton and O'Neill, 2002; Golightly and Wilkinson, 2005).

A big hurdle facing further statistical development for processes on networks is the lack of sufficient high quality time-index network data, to make sensible statistical inferences. We find that GPS data can provide such quality. This paper proposes a novel statistical inference and prediction methods that can be used to model travel time on real-world networks, and similar processes on

---

<sup>1</sup>As examples, Google Maps (<https://maps.google.com>), Lyft Inc., and Uber Inc.

dynamical networks. We adopt transportation lexicon for easier readability.

Section 3.1 characterizes transportation networks as a directed graph with stochastic edge-speed, by means of integrating important properties of real-world travel time. In Section 3.1 we introduce general forms of dependencies between sequences of random variables to capture spatial and temporal dependencies in travel time. Under mild regularity conditions, Section 4.1 shows that without assuming a distribution for speed,  $\mathcal{T}_\rho$  can be normalized to a standard normal distribution. Oppenlander (1976) was the first to suggest such a possibility in real-world transportation networks, yet the problem remained open until now. We also provide efficient methods to estimate the parameters of the asymptotic distribution. We propose two types of prediction intervals for single trips in Section 5. The first interval uses the estimates of the universal parameters directly. The second interval uses trip-specific parameters that enable more tailored and tighter intervals. We report the results of a real-world case study using GPS data collected from mobile phones in Quebec City in Section 6 and show that our proposed approach compares favorably to previous empirical approaches for travel-time estimation.

## 2 Transportation networks

### 2.1 Network notations

We define a transportation graph  $G = (N, E, D)$  as a directed connected graph consisting of a finite *node* set  $N$  and an *edge* set  $E$ . For each edge  $e \in E$ ,  $d_e \in D$  defines the edge traversal positive distance.  $G$  is connected in the sense that there exist a traversable route between any two nodes of  $G$ . A *route*  $\rho$  in  $G$  consists of an  $n$ -sequence of connected edges  $\rho = \langle e_1, e_2, \dots, e_n \rangle$  that define the order of travel. We distinguish a route  $\rho$  in  $G$  by the angle bracket  $\langle \cdot \rangle$ , such that  $\langle e, e' \rangle \in \rho$  is a subroute composed of a pair of edges  $e$  and  $e'$ .  $\langle \dots, e \rangle$  refers to a subroute in  $\rho$ , up to and including, edge  $e$ .  $n = \#\{e : e \in \rho\}$  refers to the length (number of edges) of  $\rho$  and  $n_e$  to the number of time edge  $e$  appears in  $\rho$ . Without loss of generality, we assume that the endpoints of  $\rho$  are traveled in full. In practice, the actual traveled distance can be used instead.

### 2.2 Distribution of speed

Let the continuous map  $(s, t) \mapsto F_e(s, t)$ , in both  $s$  and  $t$ , represent the cumulative distribution function (CDF) of the reciprocal of speed  $S_e$ , for every time index  $t > 0$ .

The function  $F_e(\cdot, t)$  is a strictly increasing function. A random speed observation at time  $t_0$  can be defined by its inverse CDF as  $S_e(t_0) = F_e^{-1}(U, t_0)$ , where  $U$  is a Uniform[0, 1] random variable and  $F^{-1}$  is the inverse CDF. The temporal distribution of speed on the network  $G$  can be represented as

$$(S_e(t), e \in E) \stackrel{d}{=} (F_e^{-1}(U_e, t), e \in E), \quad (U_e, e \in E) \stackrel{i.i.d.}{\sim} \text{Uniform}[0, 1], \quad (2)$$

where  $\stackrel{d}{=}$  implies equality in distribution. In real-world transportation networks  $(S_e, e \in E)$  are strictly positive and bounded random variables, since they cannot be zero over an edge with positive length. Moreover, speed on an edge has strong seasonal patterns, or what is more known as cyclostationarity process (Gardner et al., 2006). Hence, we define  $S_e$  under the following assumptions.

**Assumption 1.** *For a time index  $t > 0$ , suppose that the distribution of speed  $S_e(t)$  over an arbitrary edge  $e \in E$  is in the wide sense cyclostationarity*

$$S_e(t) = m_e(t) + \epsilon_e(t), \quad (3)$$

where  $S_e(t) \in \mathcal{C}_e = [\delta_e, M_e]$  for some  $0 < \delta_e < M_e < \infty$ ;  $m_e(t) = \mathbb{E}[S_e(t)]$  and  $\sigma_e^2(t) = \mathbb{E}[\epsilon_e^2(t)] > 0$  are continuous cyclostationarity functions with respect to  $t$ ; with  $\mathbb{E}[\epsilon_e(t)] = 0$  for all  $t > 0$ .

In the side sense cyclostationarity is what refer to as the cyclostationarity of  $m_e(t)$ , and  $\sigma_e(t)$ , which is not practically necessary from an inference perspective, since speed is bounded. However, to make sensible predictions, which is one the aim of this paper, some form of structure is required. Seasonality of  $m_e(t)$  is also justified from the periodic empirical behavior of speed in real-world networks, discussed in various forms (Jenelius and Koutsopoulos, 2013; Zheng and J van Zuylen, 2013; Wang et al., 2019; Woodard et al., 2017). In real-world networks, it is possible that there exists multiple periodic trends for the same edge  $e$  and this can be modeled additively through the mean  $m_e(t)$ .

Periodicity of speeds on edges are timely coordinated over large areas of real-world networks. This is a consequence of traffic density in the network, and one example is morning (evening) rush hours (Treiber et al., 2000; Geroliminis and Daganzo, 2008). In a methodological sense, we refer to such timely and wide-spread patterns as *speed regimes*, and we assume that they have a causal effect on the distribution of speed over the network. By this causal relationship we can decouple the dependencies of speed over adjacent edges as follows.

**Assumption 2.** *There exist a latent random variable  $t \mapsto \Pi(t)$ , with continuous sample path with respect to  $t > 0$ , such that  $S_e \perp\!\!\!\perp S_{e'} \mid \Pi$  for distinct edges  $e, e' \in E$ , for all times  $t > 0$ .*

We refer to  $G = (N, E, D, S)$ , where  $S = (S_e(t), e \in E)$ , as a transportation network whenever Assumptions 1 and 2 are satisfied. Assumption 2 is not directly used in the text but a part of the proof of Theorem 6. The next section builds on the assumed distribution of speed over an edge of this section, to characterizes the distribution of speed over a route (in a trip's view) in  $G$ .

### 3 Travel time as a random variable

#### 3.1 Dependency in travel time

The main difficulty in inferring the distribution of  $\mathcal{T}_\rho$ , in the real-world, is the different sources of dependencies affecting the distribution of  $(S_e, e \in \rho)$ , which we summarize in two categories, i) *within-trip (serial) dependency* which refers to the dependency between speed on consecutive edges within the same trip (a trip view); and ii) *filtration (time) dependency* which refers to the fact that, from a trip view, the distribution of speed at an edge depends on the arrival time at that edge, and hence on the travel time up to that edge. Otherwise, by continuity and boundedness of speed (assumption 1), it can be approximated by a Gaussian mixture (Norets, 2010; Ghosh et al., 2003)). The variability of such measurement can be large, and precise information on the speed distribution at a future time  $t$ , depends on  $t$ .

To further understand the structural difference between time and serial dependency, let  $(U_e, e \in \rho)$  define a sequence of serially dependent Uniform[0,1] random variables. Then a trip's distribution of speed over a route  $\rho$  is then

$$(S_e, e \in \rho) \stackrel{d}{=} (F_e^{-1}(U_e, \tau_e), e \in \rho), \quad (4)$$

where times  $(\tau_e, e \in \rho)$ , represent the arrival time at edge  $e$ , defined by the recursive map

$$\tau_e = \tau_{e'} + d_{e'} S_{e'}(\tau_{e'}), \quad \langle e', e \rangle \in \rho. \quad (5)$$

We use the notation  $\tau_e$ , rather than  $t_e$ , since the former is a random time. The map 5 is referred to as rotation mapping in dynamical systems literature, see Einsiedler and Ward (2013, Prop 2.16), and Appendix Example 5.

The main difference between (2) and (4) is that the latter captures extra dependencies associated with vehicle behavior. For example, in the real-world, on non-congested highways, a driver that tends to drive faster than average speed can sustain such behavior longer. We refer to this form of dependency as within-trip dependency, and associate it with the serial dependencies in  $(U_e, e \in \rho)$ . (2) marginalizes out the vehicle behaviour to look at the (unconditional) distribution of speed from the network perspective.

Filtration dependency arise from the dependency of speed distribution on time  $\tau_e$ , as in (4), and is captured by the recursive map in (5). It consequently affects the variability in  $F_e(\cdot, t)$  across time. In the real-world, filtration dependency is induced by factors, such as congestion. For example, at night, it is safe to assume that all roads are fairly empty, resulting in a time-invariant  $F_e$  for that period. On the other hand, filtration dependency is strongest in high-traffic time. Traffic and network topology both have a causal effect on filtration and within-trip dependencies. We pair " $e \in \rho$ " with a random variable to refer to the conditional version, as in (4), as opposed to " $e \in E$ ",

for unconditional version, in (2). We also assume no across-trip dependency, in other words trips are independent from each other.

The next section introduces a more rigorous, although general, form of serial dependency assumed for  $(U_e, e \in \rho)$ . With the filtration dependency in (5), the section also formalizes travel time as a sampling process over  $G$ .

### 3.2 Travel-time as a sampling process

Dependency of random variables cannot be measured without knowing the true generating distribution, and real-world travel time is empirical in nature. Nonetheless, it is widely accepted, and empirically shown in many studies, that within-trip dependency decreases with distance; see for example [Woodard et al. \(2017, Figure 5\)](#). Sequences of random variables that exhibit such form of serial dependency, variables far apart are nearly independent, are referred to as *mixing* sequences. Different mixing types have been introduced in probabilistic literature, each with their measuring coefficients. Refer to [Bradley \(2005\)](#) for a concise survey on this topic. The most general, in a sense implied by many other types, is called  $\alpha$ -mixing (strongly mixing) and is defined below ([Rosenblatt, 1956](#)).

**Definition 1.** Let  $(X_k, k \in \mathbb{Z})$  be a sequence of random variables defined on the probability space  $(\Omega, \mathcal{F}, P)$ . Define the  $\sigma$ -algebra  $\mathcal{F}_a^b$  as  $\mathcal{F}_a^b = \sigma(X_k, a \leq k \leq b, k \in \mathbb{Z}), \quad 1 \leq a \leq b \leq \infty$ . For each  $n \geq 1$  define the measure of dependence

$$\alpha(n) = \sup_{k \geq 1} \sup_{A \in \mathcal{F}_1^k, B \in \mathcal{F}_{k+n}^\infty} |P(A \cap B) - P(A)P(B)|. \quad (6)$$

If  $\alpha(n) \rightarrow 0$  as  $n \rightarrow \infty$ , then  $(X_k, k \in \mathbb{Z})$  is said to be  $\alpha$ -mixing.

With this general mixing form of dependency, we assume that the sequence  $(U_e, e \in \rho)$ , in (4), is  $\alpha$ -mixing. Assuming a stronger and more analytical form of dependency, Markovian as an example, would have yielded a simpler and possibly more analytical models. However, empirical evidence of such dependencies are weak ([Woodard et al., 2017](#)). Since  $(S_e, e \in \rho)$  are not strictly stationary (i.e. have a time-invariant distribution), we require an extra mixing condition that is slightly stronger than, and implies, the maximal correlation coefficient (defined as  $\rho(n)$  in [Bradley \(2005\)](#)), which is related to mixing of interlaced sets.

**Definition 2.** Following 1, let  $\mathcal{F}_A = \sigma(X_i, i \in A)$  for any non-empty set  $A \subset \mathbb{Z}$ . Define the dependency measure

$$\rho^*(n) = \sup_{A, B} \sup_{f, g} |\text{Corr}(f, g)|, \quad f \in \mathcal{L}^2(\mathcal{F}_A), \quad g \in \mathcal{L}^2(\mathcal{F}_B), \quad \min_{i \in A, j \in B} |i - j| \geq n, \quad (7)$$

where  $\mathcal{L}^2(\mathcal{F}_A)$  denotes the space of square-integrable  $\mathcal{F}_A$  random variables, and the supremum is over all disjoint non-empty sets  $A, B \in \mathbb{Z}$ .

Generally, we have  $0 \leq \rho^*(n) \leq 1$ , and thus the objective of Definition 2 is to insure that there is no disjoint sets of random variables that are fully correlated. Not such a stringent condition when considering travel time, since for any collection of edges, speeds are assumed to be not fully correlated. From mixing Definitions 1 and 2, we let  $(S_e, e \in \rho)$  be sequential samples from edges in  $\rho$  over a transportation network  $G$ , such that, for a given route,  $\rho = \langle e_1, e_2, \dots, e_n \rangle$ , the sampling occurs at the random entrance times  $\tau_{e_1} < \tau_{e_2} < \dots < \tau_{e_n}$ , defined as

$$\tau_e = \min\{t > 0 : \mathcal{T}_{\langle \dots, e \rangle} \leq t\}, \quad (8)$$

or, equivalently, through the recursive relation in (5). Here  $\langle \dots, e \rangle$  is the route up to edge  $e$ . We define travel time as a random variable as follows.

**Definition 3** (Travel time random variable). *For a transportation network  $G$ , an arbitrary route  $\rho$  and a start time  $t_0$ , let  $(U_e, e \in \rho)$  be an  $\alpha$ -mixing sequence of Uniform[0,1] random variables, such that  $\sum_{n>0} n^{-1} \alpha(n) < \infty$  and  $\lim_{n \rightarrow \infty} \rho^*(n) < 1$ . Let  $U_{\langle \dots, e' \rangle} = (U_e, e \in \langle \dots, e' \rangle)$ , travel-time as a random variable is constructed as*

$$\mathcal{T}_\rho = \sum_{e \in \rho} d_e m_e(\tau) + \sum_{e \in \rho} d_e \epsilon_e(\tau), \quad (9)$$

where  $m_e(\tau) = \mathbb{E}[S_e(\tau) \mid U_{\langle \dots, e \rangle}]$ ,  $\epsilon_e(\tau) = S_e(\tau) - m_e(\tau)$ ,  $\tau_e$  as in (8).

In (9), we removed the indexing of  $\tau$  since it is already implied by the subscript of the functional. From Assumption 1, the residual  $(\epsilon_e(\tau), e \in \rho)$  are not identically distributed. They are also dependent through  $U_{\langle \dots, e' \rangle}$ , the within-trip dependency.

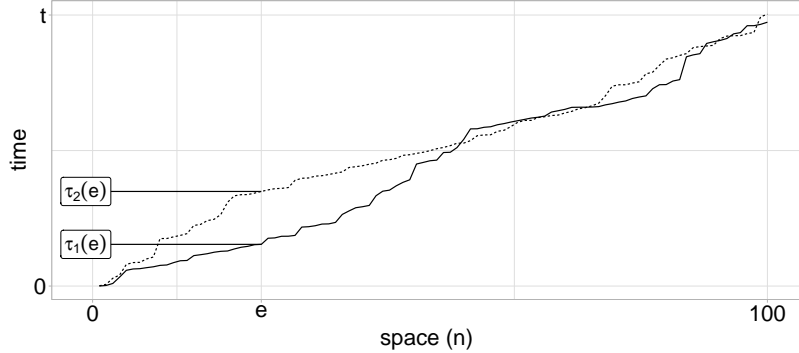


Figure 1: A toy example of two vehicles traveling a 100-edge route, starting at the same time, with  $\tau_i(e)$ ,  $i = 1, 2$ , being the vehicles random arrival times at  $e$ .

With this construction, we motivate the study of travel time through a visual example. Figure 1 illustrates a toy example of two vehicles traveling on the same 100-edges route, and starting at

a similar time. The travel time up to edge  $e$ , is clearly different for each vehicle. Yet this does not imply that the long term travel behavior of the two vehicles is different, as shown at  $e = 100$ . The short-run difference can be caused by various traffic events. Some of those events are random (unanticipated), others are deterministic, for example traffic lights. Not all deterministic events require conditioning (modeling), since many such events become noise in the long run (one example is traffic lights). This brings us to the study of long-term behavior of travel time.

## 4 Asymptotic properties of travel time

### 4.1 Asymptotic distribution

Estimating long-term behavior of the travel time defined in (3) requires proper treatment of filtration dependency. Given  $U_{\langle \dots, e \rangle}$ , the expected value of  $\mathcal{T}_\rho$ ,  $\mu_\rho(\tau)$ , is constructed by conditioning on its own stopping-times  $(\tau_e, e \in \rho)$ , as

$$\mu_\rho(\tau) = \sum_{e \in \rho} d_e \mathbb{E}[S_e(\tau) \mid U_{\langle \dots, e \rangle}] = \sum_{e \in \rho} d_e m_e(\tau) + \sum_{e \in \rho} d_e \mathbb{E}[\epsilon_e(\tau) \mid U_{\langle \dots, e \rangle}]. \quad (10)$$

The exact value of  $m_e(\tau)$  in (10) is only known at time  $\tau_e$ . Hence,  $\mu_\rho(\tau)$  is updated at each edge  $e \in \rho$ . Similarly, the variance of  $\mathcal{T}_\rho$  is

$$\sigma_\rho^2(\tau) = \sum_{e \in \rho} d_e^2 \sigma_e^2(\tau) + \sum_{e, e' \in \rho} d_e d_{e'} \mathbb{V}(\epsilon_e(\tau), \epsilon_{e'}(\tau) \mid U_{\langle \dots, e \rangle}) \quad (11)$$

where  $\sigma_e^2(\tau) = \mathbb{E}[\epsilon_e^2(\tau) \mid U_{\langle \dots, e \rangle}] - \mathbb{E}[\epsilon_e(\tau) \mid U_{\langle \dots, e \rangle}]^2$ , is the edge-level variance. We are now ready to state our first results, that the average of travel time for arbitrary routes on the network converge asymptotically to a constant that is independent from initial conditions (i.e. start time); proof in Appendix Section B

**Lemma 4.** *Under Assumptions 1, let  $\rho$  be a random walk on  $G$ . Let  $\mathcal{T}_\rho$  be as defined in 3, then  $n^{-1} \mathcal{T}_\rho \rightarrow \mu$  almost surely as  $n \rightarrow \infty$ , where  $\mu$  is the invariant expected speed defined as  $\mu = \sum_{e \in E} \pi_e \mu_e$ , with  $\mu_e = d_e \mathbb{E}[S_e] = d_e \int_{\mathcal{C}_e} m_e(t) dt$ , the unconditional average travel time over  $e$ , and  $\pi_e = n_e/n$  as  $n \rightarrow \infty$ , the stationary probability of traveling  $e$ .*

Because travel time is an empirical process, we built on the fact that  $\rho$  is a random walk on  $G$ , in Lemma 4. Many deterministic systems are essentially random walks in the limit. For example, taking a right turn on every node on a  $d$ -degree graph (every node is with  $d$ -edges) is a random walk (Aldous, 1991). If  $\rho$  is cyclical, the results still hold, since the subgraph constructed from the cycle is still a graph, and  $\mu$  would depend on it. Motivated by Peligrad (1996), we now establish a central limit theorem (CLT) for travel time, with proof in Appendix Section C.

**Theorem 5** (CLT for travel time). *Following the settings of Lemma (4), let  $\mu$  be the invariant expected travel time. Then,  $n^{-1}\sigma_\rho^2(\tau) \rightarrow \sigma^2$ , a constant. If  $\sigma^2 \neq 0$ , then*

$$n^{-1/2}(\mathcal{T}_\rho - n\mu) \xrightarrow{d} N(0, \sigma^2) \quad \text{as } n \rightarrow \infty. \quad (12)$$

Both  $\mu$  and  $\sigma^2$  are independent from initial conditions and  $\rho$ .

Regardless of start time and route, Theorem 5 states that the longer the trip is, the closer the average travel-time is to a single universal constant  $\mu$ , with universal standard deviation  $\sigma$ . The condition that  $\sigma^2 \neq 0$  is not as stringent in real-world transportation networks, since speed limits vary across edges. The next section proposes inference methods for the universal constants  $(\mu, \sigma)$ .

## 4.2 Estimation of $(\mu, \sigma)$

By cyclostationarity of  $G$ , the expected value of the average travel-time over an arbitrary route of length  $n$  is  $\mu$ , as  $\mathbb{E}[n^{-1}\mathcal{T}_\rho | n] = \mu$ , for all  $n \in \mathbb{Z}$ . This expectation is with respect to the stationary distribution  $(\pi_e, e \in E)$ . Transportation data is composed of arbitrary trips, with differing routes on the network, therefore, we treat  $n$  as a random variable. By law of total variance, the unconditional variance of average travel-time is

$$\begin{aligned} \mathbb{V}(n^{-1}\mathcal{T}_\rho) &= \mathbb{E}[\mathbb{V}(n^{-1}\mathcal{T}_\rho | n)] + \mathbb{V}(\mathbb{E}[n^{-1}\mathcal{T}_\rho | n]) \\ &= \mathbb{E}[n^{-1}(\sigma^2 + O(n))] + \mathbb{V}(\mu) = \sigma^2 \mathbb{E}[n^{-1}] \end{aligned} \quad (13)$$

With a slight abuse of notation,  $O(n)$  represents the residual as a random variable of the average variance of travel-time, as  $n^{-1}\mathbb{V}(\mathcal{T}_\rho) - \sigma^2 = O(n)$ . The expectation is with respect to distance as  $\mathbb{E}[n^{-1}O(n)] = \sum_{n_0} \mathbb{P}(n = n_0) n_0^{-1} \mathbb{E}[O(n_0)] = 0$ , since the latter is an expectation with respect to time.

With the above two identities, given a representative independent sample of  $m$  trips  $\mathcal{T}_\rho^{(j)}$ ,  $j = 1, \dots, m$ , with  $n_j$  edges each, an estimator of  $\mu$  is

$$\hat{\mu} = \frac{1}{m} \sum_{j=1}^m \frac{\mathcal{T}_\rho^{(j)}}{n_j}. \quad (14)$$

By conditioning on  $n_j$ , with the laws of total expectation and variance, we have that  $\mathbb{E}[\hat{\mu}] = m^{-1} \sum_{j=1}^m \mathbb{E}[\mathbb{E}[n_j^{-1}\mathcal{T}_\rho^{(j)} | n_j = n]] = \mu$ , and

$$\begin{aligned} \mathbb{V}(\hat{\mu}) &= \mathbb{E}[\mathbb{V}(\hat{\mu} | n)] + \mathbb{V}(\mathbb{E}[\hat{\mu} | n]) \\ &= \frac{1}{m^2} \sum_{j=1}^m \mathbb{E}\left[\frac{1}{n} [\sigma^2 + O(n)]\right] + \mathbb{V}(\mu) = \frac{\sigma^2}{m} \mathbb{E}[n^{-1}]. \end{aligned} \quad (15)$$

For a fixed route length, such as  $n_j = n$  for all  $j = 1, \dots, m$ ,  $\mathbb{V}(\hat{\mu}) = \{mn\}^{-1}\sigma^2$ ; if  $n = 1$  we retrieve the classical sample mean variance  $m^{-1}\sigma^2$ . Applying the classical results on central limit theorem of the sample mean, we have

$$\sqrt{m}(\hat{\mu} - \mu) \xrightarrow{d} N(0, \sigma^2 \mathbb{E}[n^{-1}]), \quad \text{as } m \rightarrow \infty. \quad (16)$$

From (13) and  $\mathbb{E}[n^{-1}\mathcal{T}_\rho \mid n] = \mu$ , a consistent and unbiased estimator of the unconditional variance  $\sigma^2 \mathbb{E}[n^{-1}]$  is the sample variance, as

$$\hat{\mathbb{V}}(n^{-1}\mathcal{T}_\rho) = \frac{1}{m-1} \sum_{j=1}^m (n_j^{-1}\mathcal{T}_\rho^{(j)} - \hat{\mu})^2. \quad (17)$$

Since  $n_j^{-1}\mathcal{T}_\rho^{(j)}$  are independent and identically normally distributed samples from  $G$ , then  $\hat{\mathbb{V}}(n^{-1}\mathcal{T}_\rho)$  are distributed as a chi-square with  $m-1$  degrees of freedom (Casella and Berger, 2002, Thm. 5.3.1). Moreover,  $\hat{\mathbb{V}}(n^{-1}\mathcal{T}_\rho)^{-1/2}(\mu - \hat{\mu}) \xrightarrow{d} T^{(m-1)}$ , where  $T^{(m)}$  is a student-t distribution with  $m$  degrees of freedom (Casella and Berger, 2002, Sec. 5.3.2). The variance<sup>2</sup>  $\sigma^2$  in Theorem 5 represents the limit of the conditional variance  $n^{-1}\mathbb{V}(\mathcal{T}_\rho \mid n)$ , while  $\mathbb{V}(n^{-1}\mathcal{T}_\rho) = m\mathbb{V}(\hat{\mu})$  is the total variance that treats  $n$  as random quantity. Let  $\hat{\mathbb{E}}[n^{-1}] = m^{-1} \sum_{j=1}^m n_j^{-1}$ , from (17), a profile estimator of  $\sigma^2$  is

$$\hat{\sigma}_{\text{prof}}^2 = \frac{\hat{\mathbb{V}}(n^{-1}\mathcal{T}_\rho)}{\hat{\mathbb{E}}[n^{-1}]} \quad (18)$$

### 4.3 Confidence intervals

The normality result allows easy construction of confidence intervals for the average travel time  $\mu$ . For a large sample of  $m$  trips, from (16), a  $(1 - \beta)100\%$ ,  $\beta \in (0, 1)$ , confidence interval for  $\mu$  is

$$\mu \in \left[ \hat{\mu} - T_{\beta/2}^{(m-1)} \sqrt{\frac{\hat{\mathbb{V}}(n^{-1}\mathcal{T}_\rho)}{m}}, \quad \hat{\mu} + T_{1-\beta/2}^{(m-1)} \sqrt{\frac{\hat{\mathbb{V}}(n^{-1}\mathcal{T}_\rho)}{m}} \right], \quad (19)$$

where  $\hat{\mu}$  as in (14),  $\hat{\mathbb{V}}(n^{-1}\mathcal{T}_\rho)$  as in (17), and  $T_\beta^{(m)}$  is the  $\beta$ -quantile of a student-t distribution with  $m$  degrees of freedom. For very large  $m$ ,  $T_\beta^{(m)} \approx z_\beta = \inf\{x \in \mathbb{R} : 1 - \Phi(x) > \beta\}$ , where  $\Phi(x)$  is the cumulative distribution function of a standard normal random variable.

---

<sup>2</sup>By assuming weak stationarity of the variance, following the argument of Herrndorf (1983, page 99), the variance can be represented as  $\sigma^2(n) = nh(n)$ , where  $n$  is the length of the route, and  $h(n)$  is a slow varying function. By Karamata representation theorem for slow varying function,  $h$  can be represented as  $h(n) = \exp(f(n) + \int_0^n t^{-1}g(t)dt)$ , for two bounded measurable functions  $f$  and  $g$ , where  $f(n)$  converges to a constant and  $g(n)$  to zero, as  $n \rightarrow \infty$ . This constitute an alternative approach to modeling the variance.

## 5 Prediction intervals for travel time

### 5.1 Pool-based asymptotic prediction intervals

From (12), we know that  $\mathbb{V}(\mathcal{T}_\rho^{\text{new}}) = n\sigma^2$ . When the mean and variance are known, the  $(1 - \beta)100\%$  intervals of  $N(n\mu, n\sigma^2)$  distribution can be used as a prediction interval. When the mean is unknown and the predictor of  $\mathcal{T}_\rho^{\text{new}}$  is  $n\hat{\mu}$ . A prediction interval must take into account predictor uncertainty (Geisser, 1993). The route-length conditional variance is  $\mathbb{V}(\mathcal{T}_\rho^{\text{new}} - n\hat{\mu} \mid n) = n\sigma^2(1 + m^{-1})$ . Using the profile estimator  $\hat{\sigma}_{\text{prof}}^2$  of (18), we have  $\hat{\mathbb{V}}(\mathcal{T}_\rho^{\text{new}} - n\hat{\mu} \mid n) = n\hat{\sigma}_{\text{prof}}^2(1 + m^{-1})$ . By accounting for predictive uncertain, a point-wise asymptotic prediction intervals is of the form

$$\mathcal{T}_\rho^{\text{new}} \in \left[ n\hat{\mu} - z_{\beta/2} \sqrt{n\hat{\sigma}_{\text{prof}}^2(1 + \frac{1}{m})}, \quad n\hat{\mu} + z_{1-\beta/2} \sqrt{n\hat{\sigma}_{\text{prof}}^2(1 + \frac{1}{m})} \right]. \quad (20)$$

By conditioning the variance estimate on  $n$ , (20) is a pooled interval, in the sense that it will cover with  $(1 - \beta)\%$  level of significance any arbitrary route of  $n$  edges from the pool of routes of that length. It is possible to replace  $n$  with actual unit distance (i.e. 100 meters), see the discussion in Section 7.

To use (20) for route-specific (and possibly time) non-pooled prediction intervals, one would need  $m$  independent trip samples of the route (and time) to calculate the parameters  $\hat{\mu}, \hat{\sigma}_{\text{prof}}^2$  used in (20). The next section proposes an alternative approach.

### 5.2 Trip-specific prediction intervals

Most applications are interested in bounding travel-time by constructing predictive intervals. Different types of intervals are suitable for different objectives. Network-pooled estimators, as in the universal parameters  $(\mu, \sigma)$  of Section 4.2 provide asymptotic bounds in (20) that are wider on the short-term and converges to zero in the long-term. This section provides predictive interval sequences that are trip-specific, tighter on the short-term but whose length does not converge to zero as  $n \rightarrow \infty$ .

One possible consistent estimate of  $\mu$  that can capture short-term behaviors is a recursive estimate  $\mu_\rho(t^*)$ , defined similarly to (10), although at the deterministic mean cumulative travel-times  $t^* = (t_e^*, e \in \rho)$ . Calculated recursively as in (5), as

$$t_e^* = t_{e'}^* + d_{e'} m_{e'}(t_{e'}^*), \quad \langle e', e \rangle \in \rho. \quad (21)$$

We use  $t$  rather than  $\tau$  to refer to the deterministic nature of  $t^*$ . Assuming an entrance time  $t_0$  at the first edge,  $\mu_\rho(t^*)$  is defined as

$$\mu_\rho(t^*) = \sum_{e \in \rho} m_e(t^*). \quad (22)$$

The cumulative travel-times  $(t_e^*, e \in \rho)$  can also be used to construct a covariance sum similar to the one in (11). This requires the estimation of  $2^{-1}n(n+1)$  terms:  $n$  edge  $\times$  time specific variances and  $2^{-1}n(n-1)$  pairwise correlation coefficients. This is a daunting task. A reduced covariance sum that only requires  $n+1$  parameters can be used instead, such as

$$\sigma_\rho^2(t^*) = \sum_{e \in \rho} d_e^2 \sigma_e^2(t^*) + 2\xi_G \sum_{\langle e, e' \rangle \in \rho} d_e d_{e'} \sigma_e(t^*) \sigma_{e'}(t^*), \quad (23)$$

where  $\xi_G$  is a proxy to the average lag-one auto-correlation over  $G$ , and  $\sigma_e(t^*)$  is the variance at the deterministic times in (21).

From (22) and (23), we define the asymptotic predictive distribution of travel-time. Predictive in a sense that it predicts the distribution of a trip apriori, and thus contains an added noise source resulting in an extra variance.

**Theorem 6** (Predictive distribution of  $\mathcal{T}_\rho$ ). *Following the settings of Lemma 4, let  $\mu_\rho(t^*)$  be as in (22) and  $\sigma_\rho(t^*)$  as in (23), then*

$$\sigma_\rho^{-1}(t^*) (\mathcal{T}_\rho - \mu_\rho(t^*)) \stackrel{d}{=} \sqrt{\eta} N(0, 1 + \tilde{\sigma}^2) \quad \text{as } n \rightarrow \infty, \quad (24)$$

where  $\eta$  is a strictly positive constant representing the ratio of  $n\sigma^2$  to  $\sigma_\rho^2(t^*)$ , and

$$\tilde{\sigma}^2 = \mathbb{E}[\mathbb{V}(m_e(t) \mid e)] = \sum_{e \in E} \pi_e \left[ \int_{\mathcal{C}_e} m_e^2(t) dt - \left( \int_{\mathcal{C}_e} m_e(t) dt \right)^2 \right].$$

The results in (24) require more parameter estimates than the two parameters in Theorem 5. The benefit of this approach is that i) both  $\mu_\rho(t^*)$  and  $\sigma_\rho(t^*)$  are estimable at the start of a trip, unlike (10) and (11) that are progressively updated at every edge, and ii) they result in a tighter short-term prediction sequences.

Let  $(\{\hat{m}_e, \hat{\sigma}_e^2\}, e \in \rho)$  be edge-level sample means and variances of  $m_e(t^*)$  and  $\sigma_e(t^*)$ , respectively, at times  $(t_e^*, e \in \rho)$  for a route  $\rho$ . An estimator of  $\mu_\rho(t^*)$  is

$$\hat{\mu}_\rho(t^*) = \sum_{e \in \rho} \hat{m}_e(t^*). \quad (25)$$

Given  $m$  representative independent sample of trips  $\mathcal{T}_\rho^{(j)}$ ,  $j = 1, \dots, m$ , from  $G$ , with route  $\rho^{(j)}$  of  $n_j$  length each, a pool estimator of  $\xi_G$  is

$$\hat{\xi}_G = \frac{1}{m} \sum_{j=1}^m \frac{1}{n_j} \sum_{\langle e, e' \rangle \in \rho^{(j)}} \frac{(S_e^{(j)}(\tau) - \hat{m}_e(\tau))(S_{e'}^{(j)}(\tau) - \hat{m}_{e'}(\tau))}{\hat{\sigma}_e(\tau) \hat{\sigma}_{e'}(\tau)}. \quad (26)$$

$\mathcal{T}_\rho^{(j)}$  are already observed, thus  $(\tau_e, e \in \rho^{(j)})$  in (26) are deterministic times, representing the observed entry time in each edge. A profile estimator of  $\sigma_\rho(t^*)$ , profiled at  $\hat{\xi}_G$ , is

$$\hat{\sigma}_\rho^2(t^*) = \sum_{e \in \rho} d_e^2 \hat{\sigma}_e^2(t^*) + 2\hat{\xi}_G \sum_{\langle e, e' \rangle \in \rho} d_e d_{e'} \hat{\sigma}_e(t^*) \hat{\sigma}_{e'}(t^*). \quad (27)$$

Even though  $\eta$  and  $\tilde{\sigma}^2$  in (24) are well defined quantities, their estimators can be hard to compute. A classical sample variance estimator can be used for the conditional variance of  $\mathbb{V}(m_e(t) \mid e)$  if large amounts of data per edge at time  $t$  is available. Otherwise, one requires smoothing or time binning. Therefore we propose a pooled estimator of the total total variance  $\nu = \eta(1 + \tilde{\sigma}^2)$  based on the sample variance of the residual of different trips, as

$$\hat{\nu} = \frac{1}{m-1} \sum_{j=1}^m (\varepsilon^{(j)} - \bar{\varepsilon})^2, \quad (28)$$

where  $\varepsilon^{(j)} = \{\hat{\sigma}_\rho^{(j)}(t^*)\}^{-1}(\mathcal{T}_\rho^{(j)} - \hat{\mu}_\rho^{(j)}(t^*))$ , and  $\bar{\varepsilon} = m^{-1} \sum_{j=1}^m \varepsilon^{(j)}$ . Both  $\hat{\nu}$  and  $\hat{\xi}_G$  are pooled estimators, not trip specific. By adding higher order covariance terms to the sum in (23), it is possible to reduce the variability resulting from pooling in  $\hat{\nu}$ . This approach leads to introducing an additional auto-correlation parameter; thus, its utility is application specific.

From Theorem 6, the estimators (26) and (28), a  $100 \times (1 - \beta)\%$  prediction interval for a new trip is

$$\mathcal{T}_\rho^{\text{new}} \in \left[ \hat{\mu}_\rho(t^*) - z_{\beta/2} \sqrt{\hat{\nu} \hat{\sigma}_\rho(t^*)}, \quad \hat{\mu}_\rho(t^*) + z_{1-\beta/2} \sqrt{\hat{\nu} \hat{\sigma}_\rho(t^*)} \right]. \quad (29)$$

## 6 Quebec City case study

### 6.1 Data

We use GPS data collected in 2014 by individuals located in Quebec City (Canada). Our initial Quebec City Data (QCD) contain 21,872 individual trips from over 4,000 drivers. However, no signal is given regarding the validity of each trip; i.e. if they are composed solely from motorized vehicles, excluding walkers, bikers, and non-traffic interruptions. Since our focus is on personal vehicular travel, we partition trips based on recommendations from [Woodard et al. \(2017\)](#) to remove non-motorized trips, or portions of them. Please refer to Appendix Section E.1 for the details of this data cleaning process. It is possible that some of the remaining trips are from buses or other transit modes. This is an unavoidable challenge when relying only on mobile phone location data.

Trips are composed of a sequence of GPS readings; the total trip duration is the difference between the first and last GPS timestamps. The final dataset contains 20,554 trips with median and

average duration of 19min and 21min, respectively, and a maximum of 3h27min. The median trip distance is 14.5km, mean of 16.6km and maximum of 170.4km. Median and average times between consecutive GPS observations is 4s and 9s, respectively.

We use a third-party service (TrackMatching<sup>3</sup>) to map trips GPS observations to the road network of Quebec City created by The OpenStreetMap Project (OSM);<sup>4</sup> a publicly accessible open source project. This process is called map-matching, with numerous high-quality methods (Newson and Krumm, 2009; Hunter et al., 2013). For each trip, the third-party service returns a sequence of mapped GPS points with length equal to the original sequence. Each mapped GPS point is associated with a source “node id”, “way id”, and destination “node id”, corresponding to a unique directional edge having “way id” between the source and destination nodes. The map-matching process resulted in 46,386 unique directional edges, which constitute the traveled portion of Quebec City, not the entire network. For each trip, total travel-time per edge was computed using the method described in Appendix Section E.1.

Figure 2 shows seasonal (weekly) traffic patterns per hour of week. The volume of traffic is reduced overnight in weekdays starting after 7PM, and during weekends. Daily traffic peaks are associated with AM and PM rush hours, with strong dips in between.

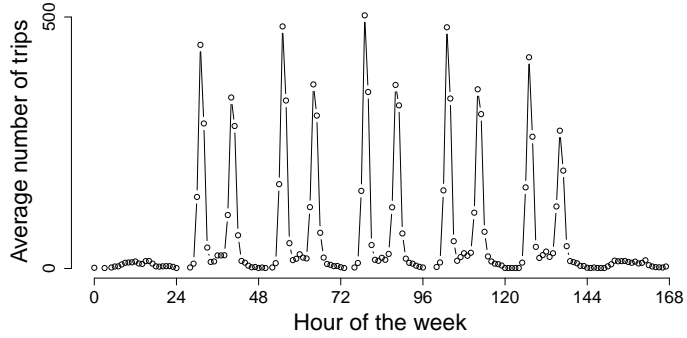


Figure 2: Average number of trips per hour in QCD, by hour of the week.

We start by exploring the data including sampling and time-binning strategies in Section 6.2. Sections 6.3 and 6.4 evaluate the pool-based and trip-specific prediction intervals. We end by comparing the out-of-sample performance of our method against previous proposed methods for travel-time estimation in Section 6.5.

---

<sup>3</sup><https://mapmatching.3scale.net>

<sup>4</sup><https://www.openstreetmap.org>

Table 1: Parameter estimation under different sampling methods

	At random	Sampling method	
		Stratified by traffic-bins	
		AM	Non-rush
$\hat{\mu}$	16.70 (16.4, 17.1)	17.90	13.70
$\hat{\mathbb{V}}(n^{-1}\mathcal{T}_\rho)$	33.50	52.90	23.00
$\hat{\mathbb{E}}[n^{-1}]$	0.02	0.02	0.02
$\hat{\sigma}_{\text{prof}}$	41.80	52.80	33.00

## 6.2 Parameter estimation

Estimating the parameters of Section 4.2 depends on the sampling method of trips. Because of the seasonal traffic pattern illustrated in Figure 2, and the sparsity of GPS data per edge, we compare our results for two sampling methods: i) sampling at random, ii) sampling stratified by three traffic time-bins (traffic-bins). Traffic-bins are discerned from Figure 2, as an i) “AM”-rush-hour bin for weekdays 6:30-8:30AM; a ii) “PM”-rush-hour bin for weekdays 3:30-5PM, and an ii) “Non-rush” bin for all remaining time periods. Alternative traffic-bins have been tested but we found that aggregating data in those bins yielded the best results. In QCD, 37% of trips occurred in an AM rush hour, with similar proportion for the PM rush hour, and 26% in all other times.

Under the random sampling method, 1000 trips are drawn to estimates the parameters of interest with results reported in Table 1. In parenthesis are the 95% confidence intervals for  $\hat{\mu}$ , calculated according to (19). For the stratified sampling method, we used 500 trips from each substrata (AM, and Non-rush) to estimate the parameters. We classify a trip into a bin if all edges are travelled within that bin (trips overlapping two traffic-bins were removed from the analysis). For numerical results on other stratas refer to Appendix Table S5.

The empirical ergodicity of the system is illustrated in Appendix Figure S5 showing that space and time averaging are almost exact for all length  $n$ , well within the 95% confidence intervals in Table 1.

## 6.3 Pool-based asymptotic prediction intervals

To illustrate the asymptotic coverage of our pool-based PI of Section 5.1, Figure 3 (left panel) reports the empirical coverage levels (dashed lines) at the theoretical 95% levels for each length  $n$ , for 500 test trips sampled at random. Our pool-based PI in (20) in solid, with progressive averages  $(n^{-1}\mathcal{T}_\rho)$  in gray for each of the 500 trips. The empirical coverage level matches the theoretical 95% level of significance for almost the whole range. Results for different stratas are similar (see Appendix Fig. S7).

To illustrate the distributional fit, Figure 3 (right panel) reports the histogram of the normalized

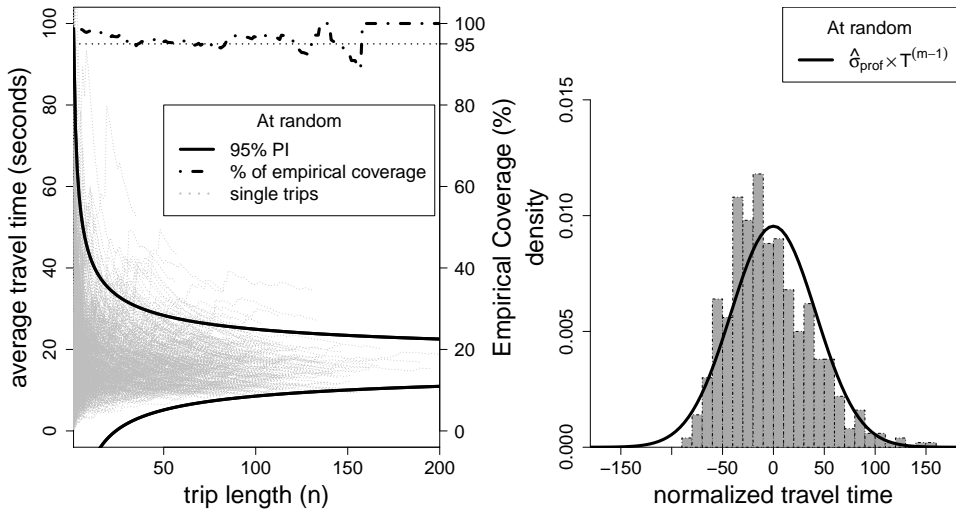


Figure 3: Average ( $n^{-1}\mathcal{T}_\rho$ ) and normalized ( $(n + nm^{-1})^{-1/2}(\mathcal{T}_\rho - n\hat{\mu})$ ) travel time for 500 test trips, sampled at random, plotted on the left and right panels, respectively. PIs of (20) are in solid. Empirical coverage levels, for each  $n$ , are in dotted lines (left panel). Right panel prediction density  $\hat{\sigma}_{\text{prof}}T^{(m-1)}$  is in solid line. Prediction parameters are in Table 1.

Table 2: Model assessment under different sampling methods for the asymptotic method. All metrics are in seconds, if not a percentage

	At random	Stratified sampling by traffic bins	
		AM	Non-rush
Root mean-squared error	379.94	383.43	288.10
Mean absolute error	285.09	289.79	194.26
Mean error	-17.56	-47.36	-6.17
Mean absolute percentage error (%)	26.83	26.59	23.38
Empirical coverage (%)	94.20	97.80	95.60
PI length	1388.1	1760.2	1022.3
PI relative length (%)	140.5	167.9	137.1

travel time  $(n + nm)^{-1/2}(\mathcal{T}_\rho - n\hat{\mu})$  for the 500 test trips, and the predictive density  $\hat{\sigma}_{\text{prof}} T^{(m-1)}$ . The value of  $n$  is trip specific, while  $m$  is the number of samples used for parameter estimation of Table 1 (500). The distributional fit varied between stratas, where the random sampling, PM and Non-rush stratas (Appendix Fig. S7), resulted in better distributional fit than the AM strata, even though the coverage probability is similar. Such discrepancy in fit is the result of the asymptotic nature of the PI. Single-edge speed is known to be heavy skewness towards lower speeds, which is discussed extensively by [van Lint et al. \(2008\)](#); [Ma et al. \(2017\)](#), [Jenelius and Koutsopoulos \(2013\)](#), Fig. 8), [Woodard et al. \(2017\)](#), Fig. 3 & 4), and others. Skewness affects the convergence rate to limiting distributions, which is evident in the right tails of Figure 3(right panel). It happens that AM rush hour has shorted rides in average than other stratas.

Table 2 illustrates various numerical results for the same test set used in Figure 3. The average PI length, for a trip sampled at random, is 140.5% of the observed travel-time. This number converges to zero theoretically as  $n$  increases, as shown in Appendix Table S7 that reports model performance under different trip lengths, for the same test set. In summary, while the empirical coverage probability sustains the theoretical level of 95%, the average PI length drops to 92.2% of the observed travel time for trips with  $n > 120$ , in comparison of 242% for trips with  $n < 40$ . The mean absolute percentage error drops to 21.48% for trips with  $n > 120$ , from 34.8% for trips with  $n < 40$ . All metrics are in seconds if not percentage, denoted by %. For more numerical results on this relation, refer to Appendix Tables S6 and S7.

#### 6.4 Trip-specific prediction interval

As in section 6.2, we group all speed observations according to the three traffic-bins (AM, PM, and Non-rush), and calculate three estimates of the mean and variance  $\{\hat{m}_e, \hat{\sigma}_e^2\}$ , for each edge  $e$ .

Figure 4 (left panel) illustrates the trip-specific 95% prediction interval sequences (PS) in (29) in comparison to the asymptotic prediction interval (PI) in (20), for a given trip of 194 edges starting

at 7:09 AM, and traveling for 24.8km over a period of 51 minutes. The latter is using the profile estimator  $\hat{\sigma}_{\text{prof}}$  of the AM strata, which corresponds to the trip's traffic-bin. As expected, trip-specific PS lead to shorter intervals, for the same level of significance, in comparison to the PI (in solid). All parameter estimates are calculated from a training set sampled from the AM strata, with more details in Appendix Section F.

With 851 test trips in the AM strata, we calculate the normalized estimated travel time as  $\hat{\sigma}_{\rho}^{-1}(t^*)(\mathcal{T}_{\rho} - \hat{\mu}_{\rho}(t^*))$ , for each trip, and plot their histogram in Figure 4 (right panel). In dashed is the  $N(0, 1)$  density, and in solid is the  $N(0, \hat{\nu})$  density, where  $\hat{\nu}$  as in (28). 95% prediction intervals, based on the former two densities, are in vertical lines in accord with the density line, with 95% empirical coverage intervals (CI) in gray. As expected, the distributional fit of the trip-specific prediction sequences are superior to the pool-based intervals (Fig. 3).

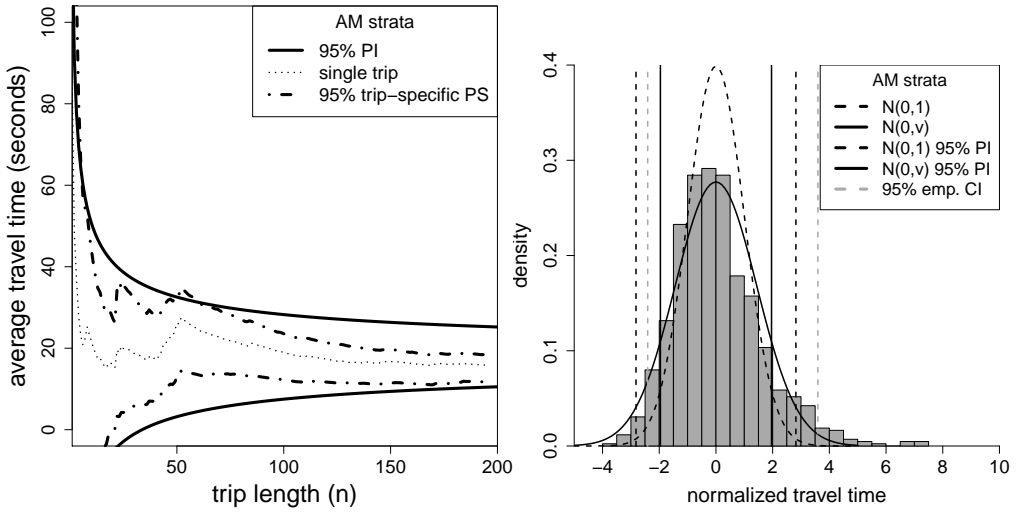


Figure 4: Trip-specific prediction sequences (PS) of a trip's average travel time  $n^{-1}\mathcal{T}_{\rho}$  (left) in comparison to the asymptotic prediction interval (PI, in solid) of (20). Histogram of normalized test trips (right) (as  $\hat{\sigma}_{\rho}^{-1}(t^*)(\mathcal{T}_{\rho} - \hat{\mu}_{\rho}(t^*))$ ) of the AM strata, with a  $N(0, 1)$  density depicted in solid,  $N(0, \hat{\nu})$  in dashed lines; 95% PI, of the former densities, are in vertical lines in accord with density line; in vertical dashed gray is 95% empirical coverage intervals (CI).

Table 3 reports additional numerical results on a test set of 2000 trips (851 AM strata, and 408 Non-rush). The estimate  $\hat{\xi}_G$  is consistently close to 0.3 across all sampling methods (with AM at 0.31, and at random 0.32). This is not surprising, since the average of  $\hat{\xi}_G$  across all trips in the training set is 0.3 (see Appendix Figure S6).  $\hat{\nu}$  estimates range between 1.31 (AM strata) to 1.45 (sampled at random), with 1.30 for Non-rush. The integration of  $\hat{\nu}$ , as a correction scalar

Table 3: Model assessment for the trip-specific method under different sampling methods. Numerical results associated with prediction intervals are listed for  $N(0, \hat{\nu})$  and  $N(0, 1)$ , separated by a comma, all metrics are in seconds, if not a percentage

	At random	Stratified sampling by traffic bins	
		AM	Non-rush
Root mean-squared error	242.17	259.58	195.28
Mean absolute error	167.60	185.83	122.89
Mean error	-1.85	8.13	-30.91
Mean absolute percentage error (%)	14.403	15.01	12.66
Empirical coverage (%)	94.6, 84.5	91.8, 82.7	92.7, 86.5
PI length	850.6, 587.3	810.6, 616.4	631.2, 454.4
PI relative length (%)	81.3, 56.1	71.4, 54.3	71.7, 51.6

to the variance in (29), improves the empirical coverage probability of the trip-specific prediction sequences by 10 percentage points. For example, with a random sampling, the empirical coverage went from 84.5% to 94.6%. Under such trip-specific method, the relative length of the PI to the trip's travel time has dropped significantly from the results of Table 2. For sampling at random, the relative PI length is 81.3%, almost half the one of the asymptotic method of 140.5%. This reduction ratio is consistent for different sampling methods. Other metrics also improved. For example, the mean error dropped from -17.56 in Table 2 to -1.85 seconds, for sampling at random.

## 6.5 Comparison to alternative models

We compare our proposed trip-specific PS to that of [Woodard et al. \(2017\)](#)<sup>5</sup>, where they used a Hidden Markov chain model(HMM) to estimate travel-time, with edge-specific states representing congestion, which we refer to as HMM. They accounted for other sources of dependency by augmenting the HMM with a trip-specific random effect, which we refer to by TRIP. We also implement a no-dependence (no-dep) model, which assumes no within-trip dependency and no random effect. Prediction intervals for TRIP, HMM and no-dep models, are in accordance with ([Woodard et al., 2017](#), Algo. 2). In particular, for each new trip, we sample 1,000 travel-times for the first edge at the start-time traffic-bin, and iteratively, for each of 1,000 samples, we sample a travel-time of the second edge at the traffic bin of the start-time plus the travel-time of the first edge, and so on until the last edge. The predictive intervals are then the empirical intervals of those 1,000 samples of total travel-time, and the prediction is the arithmetic mean of those samples.

We also compare our proposed intervals to a regression-based approach that models trip's travel time, as proposed by [Budge et al. \(2010\)](#); [Westgate et al. \(2013\)](#). In our case, we use a standard linear regression model with the log of travel- time as a response variable and total route distance

---

<sup>5</sup>R-package available at <https://melmasri.github.io/traveltimeHMM>

Table 4: Comparing trip-specific PS to alternative models; results with  $\hat{\nu} = 1$  are in parentheses

	Trip-specific PS	TRIP	HMM	no-dep	LM
Root mean-squared error	238.98	366.50	455.08	288.83	368.85
Mean absolute error	167.59	220.63	234.00	191.64	271.25
Mean error	-0.66	-55.24	-92.09	38.04	22.86
Mean absolute percentage error (%)	14.49	18.88	20.02	15.89	24.32
Empirical coverage (%)	94.75 (84.40)	89.40	82.15	73.55	96.60
PI length	855.72 (596.93)	888.93	836.19	520.92	1572.63
PI relative length (%)	80.56 (56.19)	75.90	70.02	48.53	138.02

and the traffic-bin of the trip’s start time (categorical) as predictors. The assumptions of the linear regression model hold approximately in QCD.

To estimate parameters, we sample at random 2,000 trips as a test set from QCD, and define the remaining 17,967 trips as a training set. For the trip-specific prediction sequences, we estimate edge means and variances for the three traffic-bins using the training set. Values of  $\hat{\xi}_G$  of (26) and  $\hat{\nu}$  of (28) are estimated to be 0.32 and 1.43, respectively, from a 1,000 randomly selected trips from the training set. The results of the trip-specific prediction sequences for the 2,000 test-trips are illustrated in Table 4. Parameters for the prediction intervals proposed by [Woodard et al. \(2017, Algo. 2\)](#) (TRIP, HMM and no-dep) are estimated from the same training set.

Even though TRIP and HMM improved the coverage probability in comparison to the no-dep model, they also reduce the prediction accuracy. Mean absolute percentage error for TRIP is 18.88%, it is 15.89% for the no-dep model. This pattern is consistent with the results of [Woodard et al. \(2017, Table 1\)](#). Our proposed trip-specific prediction sequences, improves the prediction accuracy and also achieves the 95% coverage level at tighter PI length (855 seconds) in comparison to TRIP (888 seconds). Our method also achieves negligible bias, -0.66 seconds of mean error.

## 7 Discussion

Our results builds on the assumption that the distribution of speed over road-segments has a periodic mean and covariance function (cyclostationarity) with respect to time. Under such assumption we establish the normality of the ratio of travel time to distance. This suggests that the empirically observed ([Woodard et al., 2017](#); [Guo et al., 2012](#)) log-normality of travel time is an artifact of the topology of the network, i.e. the distribution of distance influenced by urban planning. By conditioning on distance, travel time is at most a mixture of normals.

Without cyclostationarity, our results still hold, although for mean and variance of travel time constants that depend on the starting time initial conditions and route. Inference for such parameters can be carried, for example, by a blocking method ([Wu, 2009](#); [Peligard and Suresh, 1995](#)) given a large enough part of the trip. However, theoretical properties of such estimators are difficult to

derive.

We defined the transportation network  $G$  as a directed connected graph, where each edge represents a unique traversable edge segment. Empirically this can be defined as road-segments that have constant features along the whole segment, the endpoints of road-segments define the node set of  $G$ . Regardless of the construction, our results only depend on  $n$ , the number of traveled edges, and thus is invariant to the construction method of  $G$ . The construction method only affect the interpretation of the asymptotic location and scale parameters  $(\mu, \sigma)$ . For example, if the edges of  $G$  represent unique 100-meter segments, then  $\mu$  would represent the average travel time for an arbitrary 100-meter segment. A construction can also be trip-specific.

More generally, our work provides a limit theorem for a type of mixing processes on ergodic dynamical networks. The latter property allows for efficient inference and predictive methods. Remaining questions exist and here are a few. Given a distribution of distance, how can the limit distributions be used to simultaneously sample routes and travel time to retrieve back network dynamics mimicking that of the initial input? How to pool route variances to construct an efficient test statistic for difference of percolation regimes, i.e. travel times? How to efficiently test the hypothesis that travel-time on a route is faster and/or less variable than on an alternative route?

## References

Aldous, D. (1991). *Applications of Random Walks on Finite Graphs*, Volume Volume 18 of *Lecture Notes–Monograph Series*, pp. 12–26. Hayward, CA: Institute of Mathematical Statistics.

Barat, A., M. Barthelemy, and A. Vespignani (2008). *Dynamical processes on complex networks*. Cambridge university press.

Benjamini, I. and O. Schramm (2011). Recurrence of distributional limits of finite planar graphs. In *Selected Works of Oded Schramm*, pp. 533–545. Springer.

Berbee, H. (1987). Convergence rates in the strong law for bounded mixing sequences. *Probability theory and related fields* 74(2), 255–270.

Billingsley, P. (1965). *Ergodic theory and information*, Volume 1. Wiley New York.

Bradley, R. C. (2005). Basic properties of strong mixing conditions. a survey and some open questions. *Probab. Surveys* 2, 107–144.

Britton, T. and P. D. O'Neill (2002). Bayesian inference for stochastic epidemics in populations with random social structure. *Scandinavian Journal of Statistics* 29(3), 375–390.

Budge, S., A. Ingolfsson, and D. Zerom (2010). Empirical analysis of ambulance travel times: the case of calgary emergency medical services. *Management Science* 56(4), 716–723.

Burk, W. J., C. E. Steglich, and T. A. Snijders (2007). Beyond dyadic interdependence: Actor-oriented models for co-evolving social networks and individual behaviors. *International journal of behavioral development* 31(4), 397–404.

Casella, G. and R. L. Berger (2002). *Statistical inference*, Volume 2. Duxbury Pacific Grove, CA.

Doyle, P. G. and J. L. Snell (1984). *Random walks and electric networks*, Volume 22. American Mathematical Society.

Einsiedler, M. and T. Ward (2013). *Ergodic theory*. Springer.

Gao, X., H. Xu, and D. Ye (2009). Asymptotic behavior of tail density for sum of correlated lognormal variables. *International Journal of Mathematics and Mathematical Sciences* 2009.

Gardner, W. A., A. Napolitano, and L. Paura (2006). Cyclostationarity: Half a century of research. *Signal processing* 86(4), 639–697.

Geisser, S. (1993). *Predictive inference: An Introduction*, Volume 55. Chapman & Hall.

Geroliminis, N. and C. F. Daganzo (2008). Existence of urban-scale macroscopic fundamental diagrams: Some experimental findings. *Transportation Research Part B: Methodological* 42(9), 759–770.

Ghosh, J., R. Ramamoorthi, and Springer-Verlag (2003). *Bayesian Nonparametrics*. Springer Series in Statistics. Springer.

Golightly, A. and D. J. Wilkinson (2005). Bayesian inference for stochastic kinetic models using a diffusion approximation. *Biometrics* 61(3), 781–788.

Guo, F., Q. Li, and H. Rakha (2012). Multistate travel time reliability models with skewed component distributions. *Transportation Research Record: Journal of the Transportation Research Board* (2315), 47–53.

Herrndorf, N. (1983). The invariance principle for  $\phi$ -mixing sequences. *Zeitschrift für Wahrscheinlichkeitstheorie und Verwandte Gebiete* 63(1), 97–108.

Hunter, T., T. Das, M. Zaharia, P. Abbeel, and A. M. Bayen (2013). Large-scale estimation in cyberphysical systems using streaming data: a case study with arterial traffic estimation. *IEEE Transactions on Automation Science and Engineering* 10(4), 884–898.

Hunter, T., R. Herring, P. Abbeel, and A. Bayen (2009). Path and travel time inference from GPS probe vehicle data. *NIPS Analyzing Networks and Learning with Graphs* 12(1), 1–8.

Jenelius, E. and H. N. Koutsopoulos (2013). Travel time estimation for urban road networks using low frequency probe vehicle data. *Transportation Research Part B: Methodological* 53, 64–81.

Kallenberg, O. (2006). *Foundations of modern probability*. Springer Science & Business Media.

Keeling, M. J. and K. T. Eames (2005). Networks and epidemic models. *Journal of the Royal Society Interface* 2(4), 295–307.

Kolaczyk, E. D. (2009). Models for network graphs. In *Statistical Analysis of Network Data*, pp. 1–44. Springer.

Kolaczyk, E. D. and G. Csárdi (2014). *Statistical analysis of network data with R*, Volume 65. Springer.

Limic, V., N. Limić, et al. (2018). Equidistribution, uniform distribution: a probabilist’s perspective. *Probability Surveys* 15, 131–155.

Lo, C.-F. (2012). The sum and difference of two lognormal random variables. *Journal of Applied Mathematics* 2012.

Ma, Z., H. N. Koutsopoulos, L. Ferreira, and M. Mesbah (2017). Estimation of trip travel time distribution using a generalized markov chain approach. *Transportation Research Part C: Emerging Technologies* 74, 1–21.

Newson, P. and J. Krumm (2009). Hidden markov map matching through noise and sparseness. In *Proceedings of the 17th ACM SIGSPATIAL international conference on advances in geographic information systems*, pp. 336–343. ACM.

Norets, A. (2010). Approximation of conditional densities by smooth mixtures of regressions. *The Annals of statistics* 38(3), 1733–1766.

Oppenlander, J. C. (1976). Sample size determination for travel time and delay studies. *Traffic Engineering* 46(9).

Peligard, M. and R. Suresh (1995). Estimation of variance of partial sums of an associated sequence of random variables. *Stochastic processes and their applications* 56(2), 307–319.

Peligrad, M. (1996). On the asymptotic normality of sequences of weak dependent random variables. *Journal of Theoretical Probability* 9(3), 703–715.

Ramsay, J. O., G. Hooker, D. Campbell, and J. Cao (2007). Parameter estimation for differential equations: a generalized smoothing approach. *Journal of the Royal Statistical Society: Series B (Statistical Methodology)* 69(5), 741–796.

Rosenblatt, M. (1956). A central limit theorem and a strong mixing condition. *Proceedings of the National Academy of Sciences of the United States of America* 42(1), 43.

Snijders, T., C. Steglich, and M. Schweinberger (2017). Modeling the coevolution of networks and behavior. In *Longitudinal models in the behavioral and related sciences*, pp. 41–71. Routledge.

Tebaldi, C. and M. West (1998). Bayesian inference on network traffic using link count data. *Journal of the American Statistical Association* 93(442), 557–573.

Treiber, M., A. Hennecke, and D. Helbing (2000). Congested traffic states in empirical observations and microscopic simulations. *Physical review E* 62(2), 1805.

van Lint, J., H. J. van Zuylen, and H. Tu (2008). Travel time unreliability on freeways: Why measures based on variance tell only half the story. *Transportation Research Part A: Policy and Practice* 42(1), 258–277.

Wang, H., X. Tang, Y.-H. Kuo, D. Kifer, and Z. Li (2019). A simple baseline for travel time estimation using large-scale trip data. *ACM Transactions on Intelligent Systems and Technology (TIST)* 10(2), 19.

Westgate, B. S., D. B. Woodard, D. S. Matteson, S. G. Henderson, et al. (2013). Travel time estimation for ambulances using bayesian data augmentation. *The Annals of Applied Statistics* 7(2), 1139–1161.

Weyl, H. (1916). Über die gleichverteilung von zahlen mod. eins. *Mathematische Annalen* 77(3), 313–352.

Woodard, D., G. Nogin, P. Koch, D. Racz, M. Goldszmidt, and E. Horvitz (2017). Predicting travel time reliability using mobile phone GPS data. *Transportation Research Part C: Emerging Technologies* 75, 30–44.

Wu, W. B. (2009). Recursive estimation of time-average variance constants. *The Annals of Applied Probability* 19(4), 1529–1552.

Zheng, F. and H. J van Zuylen (2013). Urban link travel time estimation based on sparse probe vehicle data. *Transportation Research Part C: Emerging Technologies* 31, 145–157.

# Appendices

## A Technical Lemmas

The proof of the main result in this paper builds on the literature of dynamical systems and Birkhoff's Ergodic Theorem. In this section, we state general technical lemmas and definitions that are needed.

We use  $(X, \mathcal{B}, \mu)$  to refer to a probability space associated with a random variable  $X$  having a  $\sigma$ -finite Borel algebra  $\mathcal{B}$  and a probability measure  $\mu$ , such that  $\mu(X) = 1$ .

**Definition 7.** A measure-preserving system (or a dynamical system) is the quadruple  $(X, \mathcal{B}, \mu, T)$ , where  $(X, \mathcal{B}, \mu)$  is a probability space, and  $T : X \rightarrow X$  is a measure-preserving map such  $T^{-1}A \in \mathcal{B}$  and  $\mu(T^{-1}A) = \mu(A)$  for all  $A \in \mathcal{B}$ ; that is  $T$  is  $\mu$ -measurable and  $\mu$ -invariant.

$T^{-1}$  is the inverse of  $T$ . A series of measure-preserving transformations define an *orbit* around a initial point  $x_0 \in X$ , as

$$\{x_0, Tx_0, T^2x_0, \dots, T^n x_0 = T \circ T \circ \dots \circ T x_0\}.$$

**Definition 8.** Let  $(X, \mathcal{B}, \mu, T)$  be a measure-preserving system, and let  $A \in \mathcal{B}$ . We say the orbit  $(T^n x_0)_{n \geq 0}$  **equidistributes** in  $A$  if

$$\lim_{N \rightarrow \infty} \frac{1}{N} \# \{n \in \{0, 1, \dots, N-1\} : T^n x_0 \in A\} \rightarrow \mu(A) \text{ a.s.}$$

Further, we say  $T$  is **equidistributing**, if for every  $A \in \mathcal{B}$  the orbit  $(T^n x_0)_{n \geq 0}$  equidistributes in  $A$  for almost every  $x_0 \in X$ .

In a sense, the frequency distribution of the number of visits to  $A$  converges to  $\mu(A)$  almost surely.

**Definition 9.** A measure-preserving system  $(X, \mathcal{B}, \mu, T)$  is called **ergodic**, if for any  $A \in \mathcal{B}$  such that  $T^{-1}A = A$ , implies that  $\mu(A) = 0$  or  $\mu(A) = 1$ .

**Definition 10.** A measure-preserving system  $(X, \mathcal{B}, \mu, T)$  is called **mixing**, if for any  $A, B \in \mathcal{B}$

$$\lim_{n \rightarrow \infty} \mu(A \cap T^{-n}B) - \mu(A)\mu(B) = 0.$$

**Lemma 11** (Thm 1.3 [Billingsley \(1965\)](#)). On a probability space  $(X, \mathcal{B}, \mu)$ , let  $T : X \rightarrow X$  be a measure-preserving transformation. If a function  $f$  is  $L^1(X, \mathcal{B}, \mu)$ , then there exists a  $L^1(X, \mathcal{B}, \mu)$  invariant function  $g$  such that  $\int g d\mu = \int f d\mu$ , and

$$\lim_{n \rightarrow \infty} \frac{1}{n} \sum_{k=0}^{n-1} f(T^k x_0) = g(x_0) \quad \text{a.e (almost everywhere).} \quad (\text{S30.30})$$

If the system is ergodic, i.e.  $T$  is equidistributing, then  $g(x_0) = \int f d\mu$  a.e.

Essentially, ergodicity entails that the system tends to forget the initial value  $x_0$ . Lemma 11 is an adaptation of (Billingsley, 1965, Thm 1.3), thus will not be proven. To prove our results, we need the following series of lemmas and examples.

**Example 12** (Prop. 2.16 Einsiedler and Ward (2013)). *Let  $([0, 1], \mathcal{B}([0, 1]), \lambda)$  be the  $[0, 1]$  metric space equipped with the Lebesgue measure  $\lambda$ . Let  $Tx = T(x) \pmod{1} = x + \alpha \pmod{1}$ . Then, if  $\alpha \in \mathbb{R} \setminus \mathbb{Q}$  (irrationals) the system is ergodic, if  $\alpha \notin \mathbb{Q}$ , the system is not ergodic.*

Part of our results require the ergodicity and mixing of random rotation dynamical systems. The following lemma establishes the ergodicity results with proof in Section B.1.

**Lemma 13.** *Let  $([0, 1], \mathcal{B}([0, 1]), \lambda)$  be the  $[0, 1]$  metric space equipped with the Lebesgue measure  $\lambda$ . Let  $T_k x = T_k(x) \pmod{1} = x + u_k \pmod{1}$ , for  $u_k \stackrel{i.i.d.}{\sim} \text{Uniform}[0, 1]$ , then,  $([0, 1], \mathcal{B}([0, 1]), \lambda, (T_k)_k)$  is ergodic.*

We show that random rotations are also mixing in the following Lemma with proof in Section B.2

**Lemma 14.** *Under the setting of Lemma 13, random rotations are mixing in the sense of Definition 10.*

**Lemma 15** (Random rotations are random variables). *Under the setting of Lemma 13, for any  $x \in [0, 1]$ , the family  $(T^k x)_{k \geq 1} \stackrel{d}{=} (U_k)_{k \geq 1}$ , where  $(U_k)_{k \geq 1} \stackrel{iid}{\sim} \text{Uniform}[0, 1]$ . Moreover, for any function,  $f : [0, 1] \mapsto \mathbb{R}$ ,  $f \in L^2(\lambda)$  with  $\int f d\lambda = 0$ , for any  $x \in [0, 1]$ , there exist a random variable  $X_k \in \mathbb{R}$ , such that  $X_k \stackrel{a.s.}{=} f(U_k)$  for all  $k$ , with  $\mathbb{E}X_k = 0$ .*

*Proof.* Irrationals are dense in  $\mathbb{R}$ , hence an absolutely continuous random variables is almost surely irrational. By Lemmas 13 and 14  $T$  is ergodic and mixing. By construction and Kallenberg (2006, Thm. 5.10), for any  $x \in [0, 1]$ , the family  $(T^k x)_{k \geq 1} \stackrel{d}{=} (U_k)_{k \geq 1}$ , where  $U_k \stackrel{i.i.d.}{\sim} \text{Uniform}[0, 1]$ . Since  $f \in L^2(\lambda)$ , by Kallenberg (2006, Thm. 5.11), there exist a random variable  $X_k \in \mathbb{R}$ , such that  $X_k \stackrel{a.s.}{=} f(U_k)$  for all  $k$ , with  $\mathbb{E}X_k = 0$ .  $\square$

we extend Lemma 15 to mixing random variables in the following Lemma.

**Lemma 16.** *Under the setting of Lemma 13, define  $T_k x = x + u_k \pmod{1}$ , where  $u_k \sim$  are identically distributed  $\alpha$ -mixing  $\text{Uniform}[0, 1]$  random variables. Then for any function,  $f : [0, 1] \mapsto \mathbb{R}$ ,  $f \in L^2(\lambda)$  with  $\int f d\lambda = 0$ , for any  $x \in [0, 1]$ ,  $(f(T_k x))_{k \geq 1}$  are a sequence of  $\alpha$ -mixing random variables.*

*Proof.* Since  $f \in L^2(\lambda)$ , it is measurable. By the transfer probability argument in Kallenberg (2006, Thm. 5.10 & 5.11), for any  $x \in [0, 1]$ , for every  $k$ , there exist a random variable  $X_k \stackrel{a.s.}{=}$

$f(T_k x) \stackrel{a.s.}{=} f(U_k)$ , for some  $U_k \sim \text{Uniform}[0,1]$ . Hence for any  $A_k \in \sigma(X_k)$ , the  $\sigma$ -algebra generated by  $X_k$ , and  $T_k x = T_{k-1} x + u_k \pmod{1}$ ,  $u_k \in [0, 1]$ , we have

$$\begin{aligned}\mathbb{P}(\{X_1 \in A_1\} \cap \{X_n \in A_n\}) &= \mathbb{P}(\{u_k : f(T_1 x) \in A_1\} \cap \{u_n : f(T_n x) \in A_n\}) \\ &= \mathbb{P}(\{u_k : T_1 x \in f^{-1}(A_1)\} \cap \{u_n : T_n x \in f^{-1}(A_n)\}) \\ &= \mathbb{P}(\{u_k : T_1 x \in \bar{A}_1\} \cap \{u_n : T_n x \in \bar{A}_n\}) \\ &= \mathbb{P}(\{U_1 \in \bar{A}_1\} \cap \{U_k \in \bar{A}_n\}),\end{aligned}$$

where  $\bar{A}_k = f^{-1}(A_k) \in \sigma(T_k x)$ . Hence, if the right hand side is mixing so is the left hand side, and vice versa.  $\square$

Our proof of Theorem 6 builds on the following lemma on central limit theorem for random rotation maps.

**Lemma 17** (CLT for random rotations). *Under the setting of Lemma 13, for any function,  $f : [0, 1] \mapsto \mathbb{R}$ ,  $f \in L^2(\lambda)$  with  $\int f d\lambda = 0$ , then for any  $x \in [0, 1]$ , we have*

$$\frac{1}{\sqrt{n}} \sum_{k=1}^n f(T^k x) \stackrel{d}{=} N\left(0, \int f^2 d\lambda\right) \quad \text{as } n \rightarrow \infty.$$

*Proof.* From Lemma (15) we know that there exist a random variable  $X_k \in \mathbb{R}$ , such that  $X_k \stackrel{a.s.}{=} f(U_k)$  for all  $k$ , with  $\mathbb{E}X_k = 0$ . Hence, by classical central limit theorem Kallenberg (2006, Prop. 4.9), we have

$$\frac{1}{\sqrt{n}} \sum_{i=1}^n f(T^i x) \stackrel{d}{=} \frac{1}{\sqrt{n}} \sum_{i=1}^n X_i \stackrel{d}{=} N(0, \mathbb{E}X_1^2) \quad \text{as } n \rightarrow \infty.$$

$\square$

We state standard results from Berbee (1987).

**Lemma 18** (Thm. 1.2 Berbee (1987)). *Suppose  $(X_n, n \geq 0)$  is a sequence of  $\alpha$ -mixing bounded random variables with zero mean. If  $\sum_{n>0} n^{-1} \alpha(n) < \infty$ , then  $n^{-1} \sum_{n>0} X_n \rightarrow 0$  a.s.*

## B Proof of Lemma 4

Our proof for Lemma 4, and the main part of our analysis, is organized as follows:

1. Lemma 13 established that random rotations of the form  $Tx = x + u \pmod{1}$ ,  $u \sim \text{Uniform}[0, 1]$  are equidistributing and hence ergodic in the sense of Definition 9

2. Lemma 14 established that random rotations are also mixing in the sense of (10). In general, irrational rotations are ergodic but not mixing.
3. Lemma 15 established that random rotation dynamical systems are equal in distribution to random variable.
4. By the supremum part in the defining of  $\alpha$ -mixing in 1, we know that  $\alpha$ -mixing systems are also mixing.
5. By Lemma 16 we know that random rotation dynamical systems generated by  $\alpha$ -mixing random variables are equal in distribution to some  $\alpha$ -mixing random variable.
6. Finally, since our established dynamical system is both  $\alpha$ -mixing and random, we utilize direct probabilistic results for mixing sequences to establish a strong law of large numbers for travel time.

*Proof of Manuscript Lemma 4.* Our first condition is that  $\rho$  is a random walk on  $G$ . Without loss of generality, we will assume that every edge  $e$  has unit length (i.e.  $(d_e = 1, e \in E)$ ), thus, travel time becomes

$$\mathcal{T}_\rho = \sum_{e \in \rho} m_e(\tau) + \sum_{e \in \rho} \epsilon_e(\tau). \quad (\text{S31.31})$$

Example 12 defined  $\alpha$  as a constant, in (5) it is the random variable  $d_e S_e(t_e)$ . Hence By construction and Lemmas 14 and 15, we have that  $(\epsilon_e(\tau), e \in \rho)$  is an  $\alpha$ -mixing dynamical system with random rotations. They are  $\alpha$ -mixing since the sequence  $(U_e, e \in \rho)$  is  $\alpha$ -mixing sequence of Uniform[0,1] random variables. By Definition 3 and Lemma 18, we have  $n^{-1} \sum_{e \in \rho} \epsilon_e(\tau) \xrightarrow{a.s.} 0$ .

It remains to show that  $n^{-1} \sum_{e \in \rho} m_e(\tau)$  converges to a constant that is independent from initial conditions. By Definition 3 we know that  $G$  has a finite node set  $N$ , we denote it by  $G_N$ . By construction, transportation networks have bounded degrees  $\sup_{e \in E} \deg(e) < C_1$  for some  $C_1 < \infty$ . From Polya's Theorem on recurrence of random walks in the plane, see [Doyle and Snell \(1984, Sec. 2.14\)](#) and [Benjamini and Schramm \(2011, Thm. 1.1, Cor. 1.2\)](#),  $G$  is recurrent with probability 1 ( $G_N$  is a 2-dimensional planar graph).

Our transportation network  $G$  is equipped with random bounded weights  $(S_e, e \in E)$ . Since  $G$  is finite, and  $(S_e, e \in E)$  are bounded away from 0, then the transportation network is also recurrent with probability 1, meaning that an arbitrary long trips would return to starting edge/node with probability 1.

For each  $e \in E$ , let  $(\tau_i(e))_i$  be the the almost sure recurrent random times of  $e$ . By the recurrence property we have  $\tau_i(e) < \infty$  a.s. for all  $i \in \mathbb{Z}$ . Define  $Z_i(e) = \tau_i(e) - \tau_{i-1}(e)$  for  $i > 1$ , and  $Z_1(e) = \tau_1(e) - t_0$ , the recurrence time difference. By stationarity of  $G$ ,  $(Z_i(e))_i$  are independent stationary random variables.

We first treat each edge  $e \in E$  separately, and show that

$$\frac{1}{n_e} \sum_{i=1}^{n_e} m_e(\tau_i) \rightarrow \mu_e,$$

where  $\mu_e$  is a constant that is independent of recurrence times  $(\tau_i(e))_i$ , and  $n_e$  is the count of the latter. By continuity of  $m_e(t)$ , it is Lebesgue measurable ( $\lambda$ -measurable). Let  $a$  be the length of the seasonality cycle of  $m_e(t)$ . Then  $m_e$  is  $L^1([0, a], \mathcal{B}[0, a], \lambda)$ .

By Example 12 and Lemma 13,  $(\tau_i(e))_i$  define an equidistributing rotation mapping on the circle  $[0, a]$ , with initial point  $x_0 = t_0 + Z_1(e) \pmod{a}$ , such that

$$(\tau_i(e))_i = \left( x_0, Tx_0 = x_0 + Z_2(e) \pmod{a}, T^2x = Tx_0 + Z_3(e) \pmod{a}, \dots \right).$$

Then

$$\frac{1}{n_e} \sum_{i=1}^{n_e} m_e(\tau_i) = \frac{1}{n_e} \sum_{i=1}^{n_e} m_e(T^i x_0) \xrightarrow{n_e} \frac{1}{a} \int_0^a m_e(\lambda) d\lambda \quad (a.e.) \quad (\text{S32.32})$$

By Theorem 11,  $\int_0^a m_e(\lambda) d\lambda$  is independent of initial conditions, the  $\frac{1}{a}$  is to convert the integral to a probability. It is easy to see that

$$\frac{1}{a} \int_0^a m_e(\lambda) d\lambda = \mathbb{E}[m_e] = \mathbb{E}[\mathbb{E}[S_e(t)]] = \mathbb{E}[S_e] = \mu_e,$$

the unconditional expected speed. The Towers property was used since under stationarity,  $t$  is an index of sub- $\sigma$ -algebras  $\mathcal{F}_t \subset \mathcal{F}$ , where  $\mathcal{F}$  is the space of events of  $S$ . This is not surprising since ergodic dynamical systems have the property that space averaging equals time averaging (the sum in (S32.32)). Combining our results, we have

$$\frac{1}{n} \sum_{e \in \rho} m_e(\tau) = \sum_{e \in E} \frac{n_e}{n} \frac{1}{n_e} \sum_{i=1}^{n_e} m_e(\tau_i) \xrightarrow{n} \sum_{e \in E} \pi_e \mu_e = \mu, \quad a.s. \quad (\text{S33.33})$$

By Empirical process theory we have  $n_e/n \xrightarrow{a.s.} \pi_e \in [0, 1]$  a constant such that  $\sum_{e \in E} \pi_e = 1$ , hence  $\mu$  is the invariant expected speed over the map  $G$ .

If  $\rho$  is a simple random walk, then  $\pi_e$  would be proportional to the degree distribution of  $e$ , otherwise proportional to the weights assigned to  $e$ . We conclude the proof of Lemma 4.  $\square$

## B.1 Proof of Lemma 13

We first require a probabilistic version of Example 12, which can be deduced by the recent results of Limic et al. (2018). A general family of maps (not necessary random)  $\mathbf{T} : [0, 1] \mapsto [0, 1]$ , where

$\mathbf{T} = (T_k)_k$ ,  $T_k[0, 1] \mapsto [0, 1]$ , is sufficiently mixing to be equidistributing, if, and only if, the *Weyl criterion* (Weyl, 1916)  $W_N(\mathbf{T}, m)$  goes to 0 (Lebesgue-a.s.) as  $N \rightarrow \infty$ , where

$$W_N(\mathbf{T}, m) = \frac{1}{N} \sum_{k=1}^N \exp(2\pi i m T_k), \quad (\text{S34.34})$$

for all  $m \in \mathbb{Z} \setminus \{0\}$ . The above characterization comes from Fourier analysis. In dimension 1, the class of complex exponentials  $x \mapsto \exp(2\pi i m x)$ ,  $m \in \mathbb{Z}$  is orthonormal in  $L^2[0, 1]$ , and by the Stone-Weierstrass theorem, such class is dense in the periodic continuous functions on  $[0, 1]$  with respect to the sup-norm. Such result allows us to establish equidistributing results for probabilistic mapping. Limic et al. (2018) defined a Wely-like probabilistic criterion by defining the following random variable

$$Y_k(m) = \exp(2\pi i m T_k), \quad (\text{S35.35})$$

for random maps  $\mathbf{T} = (T_k)_k$ ,  $T_k : [0, 1] \mapsto [0, 1]$ . The following Lemma gives us condition on when a random mapping is equidistributing.

**Lemma 19** (Lem 2.2 of Limic et al. (2018)). *Let  $(T_k)_k$  be a sequence of random maps, and  $Y_k(m)$  be as in (S35.35). If for each  $m \in \mathbb{Z} \setminus \{0\}$*

$$|\mathbb{E}Y_k(m)\bar{Y}_l(m) + Y_l(m)\bar{Y}_k(m)| = O(|k - l|^\delta), \quad (\text{S36.36})$$

for some  $\delta(m) > 0$ , then  $(T_k)_k$  is completely equidistributed in  $[0, 1]$ .

Using Lemma (19), we show that the random rotation of Example 12 indexed by i.i.d uniform random numbers, such that  $T_k x = T_k(x) \pmod{1} = x + u_k \pmod{1}$ , where  $u_k \stackrel{i.i.d.}{\sim} \text{Uniform}[0, 1]$ , is equidistributing.

*Proof.* By Lemma 11 and Example 12, we know that the system is measure-preserving, to show that it is ergodic, it suffices to satisfy condition (S36.36) of Lemma 19. For any  $x \in [0, 1]$ ,  $T_1(x) = x + u_1$ , and  $T_k(x) = T_1 \circ T_2 \cdots \circ T_k(x) = x + \sum_{i=1}^k u_i$ . For each  $m \in \mathbb{Z} \setminus \{0\}$ , let  $s = \sum_{i=l}^k u_i$ , then

$$\mathbb{E}[Y_k\bar{Y}_l + Y_l\bar{Y}_k](m, x) = \mathbb{E} \left[ \exp(2\pi i m \sum_{i=l}^k u_i) + \exp(-2\pi i m \sum_{i=l}^k u_i) \right] \quad (\text{S37.37})$$

$$= 2 \int_{[0,1]^{k-l}} \cos(2\pi m s) ds \quad (\text{S38.38})$$

$$= 0 \quad (\text{S39.39})$$

□

This completes the proof of Lemma 13.

## B.2 proof of Lemma 14

To show that the mixing relation of 10 is satisfied for the space  $[0, 1] \subset \mathbb{R}$ , it is enough to show that it is satisfied for dyadic intervals, since unions of dyadic intervals form an algebra and generate all Borel sets on  $[0, 1]$ , or any  $I \subset \mathbb{R}$ . Therefore, consider the following sets

$$A = \left[ \frac{t}{2^i}, \frac{t+1}{2^i} \right], \quad B = \left[ \frac{s}{2^j}, \frac{s+1}{2^j} \right], \quad i, j \in \mathbb{N}, 0 \leq t < 2^i, 0 \leq s < 2^j.$$

Without loss of generality we will assume that  $i < j$ . Consider the random rotations  $(T_k)_{k>0}$ , where  $T_k x = x + u_k \pmod{1}$ , where  $u_k$  are i.i.d Uniform[0,1]. Then for  $i < j$ , we can find a  $u_0 \in [0, 1]$  such  $u_0 + 2^{-j}(s+1) \pmod{1} = t2^{-i}$ , in this sense, for the Lebesgue measure  $\lambda$ , we have the following 4 regions.

- for  $u_0 \leq u < u_0 + 2^{-j}$ , we have  $\lambda(A \cap [B + u \pmod{1}]) = u - u_0$ .
- for  $u_0 + 2^{-j} \leq u < u_0 + 2^{-i}$ , we have  $\lambda(A \cap [B + u \pmod{1}]) = 2^{-j}$ .
- for  $u_0 + 2^{-i} \leq u < u_0 + 2^{-i} + 2^{-j}$ , we have  $\lambda(A \cap [B + u \pmod{1}]) = (u_0 + 2^{-i} + 2^{-j} - u)$ .
- $\lambda(A \cap [B + u \pmod{1}]) = 0$  otherwise.

By change of variables we can assume that  $u_0 = 0$ , then

$$\begin{aligned} \lambda(A \cap T^{-1}B) &= \int_0^{2^{-j}} u du + \int_{2^{-j}}^{2^{-i}} \frac{1}{2^j} du + \int_{2^{-i}}^{2^{-i} + 2^{-j}} \left( \frac{1}{2^i} + \frac{1}{2^j} - u \right) du \\ &= \frac{1}{2^i} \frac{1}{2^j} = \lambda(A) \lambda(B). \end{aligned}$$

Finally, by induction the invariance property of random rotations to the Lebesgue measure, and induction, we  $\lambda(A \cap T^{-n}B) = \lambda(A) \lambda(B)$ , satisfying Definition 10. This completes the proof of Lemma 14.

## C Proof of Theorem 5

There are a few methods to prove Theorem 5. A targeted method would require the utilization of the network structure, the random walk and ergodicity of random rotations. This is a whole endeavor, and for the purpose of brevity, we rely on known central limit results for non-stationary random variables. We relate random rotation dynamical system to random variables by 15.

Let  $\{X_{ni}, 1 \leq i \leq k_n\}$  and  $n \in \mathbb{Z}$  be a triangular array of the random variables  $(X_i, i \in \mathbb{Z})$ , where  $k_n \rightarrow \infty$ . Let  $\rho_{\max}^*$  be a dependency measure between any two non-empty subsets  $A, B \subset \{1, 2, \dots, k_n\}$  of rows of the array that are at least  $k$  distance apart, as

$$\rho_{\max}^*(k) = \sup_k |\rho^*(\sigma(X_{ni}, i \in A), \sigma(X_{ni}, i \in B))|, \quad \min_{i \in A, j \in B} |i - j| \geq k. \quad (\text{S40.40})$$

**Lemma 20** (Coro. 2.1 [Peligrad \(1996\)](#)). *Let  $(X_i, i \in \mathbb{Z})$  be an  $\alpha$ -mixing sequence, with  $\mathbb{E}[X_i] = 0$  for all  $i$ , and  $(X_i^2, i \in \mathbb{Z})$  is a uniformly integrable family. Define the triangular array  $\{a_{ni}X_i, 1 \leq i \leq n\}$ , for some constants  $\{a_{ni}\}$ , and denote  $\sigma_n^2 = \mathbb{E}[(\sum_{i=1}^n a_{ni}X_i)^2]$ . Assume that*

$$\max_{1 \leq i \leq n} \frac{|a_{ni}|}{\sigma_n} \rightarrow 0, \quad \text{as } n \rightarrow \infty, \quad (\text{S41.41})$$

and

$$\sup_n \sigma_n^{-2} \sum_{k=1}^n a_{nk}^2 < \infty. \quad (\text{S42.42})$$

Assume, in addition, that  $\lim_{n \rightarrow \infty} \rho_{\max}^*(n) < 1$ , then  $\sigma_n^{-1} \sum_{i=1}^n a_{ni}X_i \xrightarrow{d} N(0, 1)$ .

*Proof of Theorem 5.* We would like to show that

$$\frac{\mathcal{T}_\rho - n\mu}{\sqrt{n}} \xrightarrow{d} N(0, \sigma^2).$$

By Lemma 4, we have that  $n^{-1} \sum_{e \in \rho} m_e(\tau) \xrightarrow{a.s.} \mu$ , where  $\mu$  is a constant. By reverse application of Slutsky's theorem, we have

$$\begin{aligned} \lim_{n \rightarrow \infty} \frac{\mathcal{T}_\rho - n\mu}{\sqrt{n}} &= \lim_{n \rightarrow \infty} \frac{\mathcal{T}_\rho - \sum_{e \in \rho} d_e m_e(\tau)}{\sqrt{n}} = \lim_{n \rightarrow \infty} \frac{1}{\sqrt{n}} \sum_{e \in \rho} d_e \epsilon_e(\tau) \\ &= \lim_{n \rightarrow \infty} \frac{1}{\sqrt{n}} \sum_{e \in \rho} d_e \sigma_e(\tau) X_e. \end{aligned}$$

Here  $(X_e, e \in \rho)$  is a sequence of  $\alpha$ -mixing random variables, having  $\mathbb{E}[X_e] = 0$ , and  $\mathbb{E}[X_e^2] = 1$  for all  $e \in \rho$ .  $\sigma_e(\tau)$  is the standard deviation of  $\epsilon_e(\tau)$ , such that  $\mathbb{V}(\epsilon_e(\tau)) = \mathbb{V}(\sigma_e(\tau)X_e) = \sigma_e^2$ . By Assumption 1,  $(S_e, e \in E)$  is a family of bounded random variables, and thus  $(S_e^2, e \in E)$  are square integrable. Moreover,  $d_e$  and  $d_e \sigma_e(\tau)$  are bounded for all  $e$  and  $\tau$ .

Since  $n^{-1} \sigma_\rho^2(\tau) \xrightarrow{a.s.} \sigma^2 \neq 0$ , in Theorem 5, it is easy to see that conditions (S41.41) and (S42.42) are satisfied. Condition  $\lim_{n \rightarrow \infty} \rho^*(n) < 1$  is assumed in Definition 3, and thus the results follow from Lemma 20.

The fact that  $\mu$  does not depend on initial conditions, follows from Lemma 4 with proof in Section B. Mainly from equidistributing (ergodicity) property of random rotations 13. Results for the second moment follow accordingly.  $\square$

## D Proof of Theorem 6

**Lemma 21.** *Following (22), let  $(t_e^*, e \in \rho)$  be defined recursively for every subroute  $\langle \dots, e', e \rangle \in \rho$  as*

$$t^*(e) = t_e^* = t_{e'}^* + d_{e'} m_{e'}(t_{e'}^*), \quad (\text{S43.43})$$

*with initial value at  $t_0$ . Then  $(t_e^*, e \in \rho)$  are equidistributing.*

*Proof.* See Section D.1 □

**Lemma 22.** *Following the settings of Lemma 21, let  $\rho$  be a random walk on a transportation network  $G$ , and define  $(t_i^*(e), i = 1, \dots, n_e)$  be the visit times to edge  $e$ . Then  $(t_i^*(e), i = 1, \dots, n_e)$  is mixing in the sense of Definition 10.*

*Proof.* See Section D.1 □

*Proof of Theorem 6.* With Theorem 5, let  $n = |\rho|$ , we decompose (24) as,

$$\frac{\mathcal{T}_\rho - \mu_\rho(t^*)}{\sigma_\rho(t^*)} = \frac{\mathcal{T}_\rho - n\mu}{\sigma_\rho(t^*)} - \frac{\mu_\rho(t^*) - n\mu}{\sigma_\rho(t^*)} = I - II. \quad (\text{S44.44})$$

By Theorem 5 and Slutsky's theorem we have,

$$I = \frac{\sqrt{n}\sigma}{\sigma_\rho(t^*)} \frac{\mathcal{T}_\rho - \mu_\rho(\tau)}{\sqrt{n}\sigma} \xrightarrow{d} \sqrt{\eta}N(0, 1), \quad \eta = \lim_{n \rightarrow \infty} \frac{n\sigma^2}{\sigma_\rho^2(t^*)}. \quad (\text{S45.45})$$

For  $II$  we will first show that  $n^{-1}\mu_\rho(t^*) \xrightarrow{a.s.} \mu$ . which requires the deterministic times  $t^* = (t_e^*, e \in \rho)$  to be equidistributing, in the sense of Definition 8. This is established by Lemmas D.1 and 13. Hence, by a similar argument to (S33.33), we have

$$\frac{1}{n}\mu_\rho(t^*) = \frac{1}{n} \sum_{e \in \rho} m_e(t^*) = \sum_{e \in E} \frac{n_e}{n} \frac{1}{n_e} \sum_{i=1}^{n_e} m_e(t_i^*(e)) \xrightarrow{n} \sum_{e \in E} \pi_e \mu_e, \quad a.s.$$

as shown in the proof of Lemma 4 in Section B,  $\rho$  is a random walk on  $G$  and hence recurrent with probability 1, see [Doyle and Snell \(1984, Sec. 2.14\)](#) and [Benjamini and Schramm \(2011, Thm. 1.1, Cor. 1.2\)](#).

Assume that the period of each  $(m_e(t), e \in E)$  is of length  $a > 0$ . Since  $m_e(t) \in L^2(\lambda)$ , and let  $(t_i^*(e), i = 1, \dots, n_e)$  be the visit times to edge  $e$  in  $(t_e^*, e \in \rho)$ . Then, by Lemma 22 the mapping  $(t_i^*(e), i = 1, \dots, n_e)$  is mixing, since it can be written as

$$t_i^*(e) = t_{i-1}^*(e) + U_i \pmod{a},$$

where  $(U_i, i = 1, \dots, n_e)$  are i.i.d Uniform $[0, a]$  random variables. By Lemma 17, for every  $e \in E$ ,

$$n_e^{-1/2} \left( \sum_{i=1}^{n_e} m_e(t_i^*) - \mu_e \right) \xrightarrow{d} N(0, \tilde{\sigma}_e^2),$$

where

$$\tilde{\sigma}_e^2 = \int_{\mathcal{C}_e} m_e^2(t) dt - \left( \int_{\mathcal{C}_e} m_e(t) dt \right)^2.$$

By Assumption 2, conditional on speed regimes  $\Pi$ , and the property of the sum of independent normal variables, we have that

$$\frac{\mu_\rho(t^*) - n\mu}{\sqrt{n}} = \sum_{e \in E} \frac{\sqrt{n_e}}{\sqrt{n}} \frac{1}{\sqrt{n_e}} \sum_{i=1}^{n_e} \left( m_e(t_i^*) - \mu_e \right) \xrightarrow{d} N(0, \tilde{\sigma}^2), \quad (\text{S46.46})$$

where, for  $n_e/n \xrightarrow{a.s.} \pi_e$ ,

$$\tilde{\sigma}^2 = \sum_{e \in E} \pi_e \sigma_e^2 = \sum_{e \in E} \pi_e \left[ \int_{\mathcal{C}_e} m_e^2(t) dt - \left( \int_{\mathcal{C}_e} m_e(t) dt \right)^2 \right].$$

By across-trip dependency  $I \perp\!\!\!\perp II$ , and from (S45.45) and (S46.46), and by a second application of Slutsky's theorem, we have

$$I + II \xrightarrow{d} \sqrt{\eta} N(0, 1) + \sqrt{\eta} N(0, \tilde{\sigma}^2), \quad \text{as } n \rightarrow \infty.$$

Moreover, at the limit, both  $I$  and  $II$  are independent of  $\Pi$ . This completes the proof of Theorem 6.  $\square$

## D.1 Proof of Lemmas 21 and 22

*Proof of Lemma 21.* Follows directly from Example 12, since for an arbitrary  $t > 0$ ,  $m_e(t)$  is almost surely irrational (by continuity), hence,  $(t_e^*, e \in \rho)$  is an irrational family of maps, thus equidistributing.  $\square$

*Proof of Lemma 22.* Following the proof arguments of Theorem 4 in Appendix B, and the fact the  $\rho$  is a random walk on  $G$ , from the recurrence property in 2-dimensional planar graphs, we have  $t_i^*(e) < \infty$  a.s. for all  $i \in \mathbb{Z}$ .

Without loss of generality, define  $U_i(e) = t_i^*(e) - t_{i-1}^*(e)$  for  $i > 1$ , the recurrence time difference, with  $U_1(e) = t_1^*(e) - t_0$ , where  $t_0$  is the start time of the trip. By stationarity of  $G$ ,  $(U_i(e), i = 1, \dots, n_e)$  are independent continuous stationary random variables. The continuity follows from the fact that  $m_e(t)$  is continuous.

By transfer probability argument in [Kallenberg \(2006, Thm. 5.10\)](#),  $(U_i(e), i = 1, \dots, n_e)$  are equal in distribution to some Uniform[0,1] random numbers. By Lemmas [14](#), let  $[0, a]$  be the cycle of edge  $e$ , then rotation mapping

$$t_i^*(e) = t_{i-1}^*(e) + U_i(e) \pmod{a},$$

is mixing. □

## E Exploratory analysis of Quebec city data

### E.1 Data preparation

Quebec city 2014 GPS data (QCD) is collected using the Mon Trajet smartphone application (developed by Brisk Synergies Inc). This study made use of a sample of open data, which contained over 4000 drivers and 21,872 individual trips. No personal identifiers of drivers were available. The precise duration of the time period is kept confidential. The application was installed voluntarily by drivers who anonymously logged trips using a simple interface.

No measure was provided to insure the validity of trips; i.e., if they are composed solely from motorized vehicles, excluding walkers, bikers, and non-traffic interruptions. The data is processed by breaking down trips into multiple trips whenever i) trips include idle time (a period of no move) of more than 4 minutes; or ii) there is more than 2 minutes between consecutive GPS observations. After decomposition, we trim end-points of trips, such that each trip starts whenever the driving speed is larger than 10km/h for the first time, and ends whenever the driving speed is less than 10km/h for the last time.

To remove non-motorized travel, we remove trips with i) median speed less than 20km/h; ii) maximum speed less than 35km/h, or iii) when driving distance is less than 1km (as measured by the sum of the great circle distances between pairs of sequential measurements). Those three requirements appear to eliminate most walking and biking travel ([Woodard et al., 2017](#)).

We estimate the total travel time per edge by calculating i) within-edge travel time, as the time spent within the edge, and ii) across-edge travel time, as the time spent crossing other edges; the time spent between the closest two GPS observations, where one is in the edge the other in the adjacent edge. In the same way we calculate across-edge distance. The total travel time per edge is then 100% of within-edge plus across-edge travel time weighted by half the proportion of across-edge distance to the total length of the edge. Total edge-lengths are obtained from OSM. In rare circumstances, the map-matching service also returns intermediate edges that do not have initial GPS observations; this happens for example when a car is driving very fast or goes through a tunnel. We treat those intermediate edges, those without GPS observations, as a single edge and calculate the total travel time over it, and then assign it proportionally to the length of each intermediate edge. With these total travel time estimates, we calculate the (reciprocal of) average speed per

edge by dividing the total travel time by total length, for fully traveled edges, and by partial lengths otherwise. Partial lengths are the distance covered by the vehicle to the traveled end-point of the edge.

## F Traffic-bin estimators

Initial cleaning of the QCD results in 19,967 trips. The data is split in a training set of 17,967 trips and a test set of 2,000 trips, the latter includes 851 trips from the AM strata, 741 from the PM, and 408 otherwise. We require at least a single observation per edge  $\times$  time bin category. Therefore, the test set is sampled randomly such that with every new sample introduced to the test set, the test set, when removed from the QCD, does not lead to edges  $\times$  time bin with no observation. The remaining trips are used as a training set.

The map-version estimators  $(\hat{m}_e, \hat{\sigma}_e^2, e \in E)$  are calculated using the training set. For each edge  $\times$  time bin, we use the average of all observations to calculate the sample mean  $\hat{m}_e$ , and similarly, we use the classical sample variance estimator to calculate  $\hat{\sigma}_e^2$ . Since all our notations use the path-conditioning ( $e \in \rho$ ), the sample mean and variance are implemented on the edge-graph and not the graph  $G$  directly. In particular, for every edge  $e$  with  $k$  exits  $\{e_1, \dots, e_k\}$  we have  $k \times \#\{\text{time bins}\}$  estimators for  $m_e$ , each represents  $\mathbb{E}[S_e(t) \mid \langle e, e_i \rangle, t \in \text{time bin}]$  and  $\mathbb{V}(S_e(t) \mid \langle e, e_i \rangle, t \in \text{time bin})$  for  $i = 1, \dots, k$ . For each trip, the notation  $(\{\hat{m}_e, \hat{\sigma}_e^2\}, e \in \rho)$  correspond exactly to the path-conditioning estimators. We use the three traffic bins introduced in section 6 to classify the time bins.

We require at least 10 observations per unit  $(\{\langle e, e_i \rangle, \text{time bin}\})$  for the estimators  $(\hat{m}_e, \hat{\sigma}_e^2, e \in E)$  to be used in practice. Approximately 90% of units have less than 10 observations. We impute those quantities in the following order; a) removing path-conditioning, i.e. impute by the M-estimate of  $\mathbb{E}[S_e(t) \mid t \in \text{time bin}]$  when  $\mathbb{E}[S_e(t) \mid \langle e, e_i \rangle, t \in \text{time bin}]$  is inestimable; and by b) removing edge-conditioning, i.e. impute by the M-estimate of  $\mathbb{E}[S(t) \mid t \in \text{time bin}]$  when a) is inestimable. Even though this imputation procedure is crude, the results are promising.

## G Additional results

### G.1 Empirical ergodicity and parameter estimation

To illustrate the empirical ergodicity of the system, Figure S5 reports the space average (dotted lines), for the portion of the first  $n$  edges, for each length  $n$ , and the time average  $\hat{\mu}$  (solid lines), for trips sampled at random (left) and by traffic-bins (right). Space and time averaging are almost exact for both sampling methods, well within the 95% confidence intervals in Table 1. In gray are the progressive averages  $(n^{-1}\mathcal{T}_\rho)$  of travel time per trip.

The following table is similar to table 1, albeit with more numerical results.

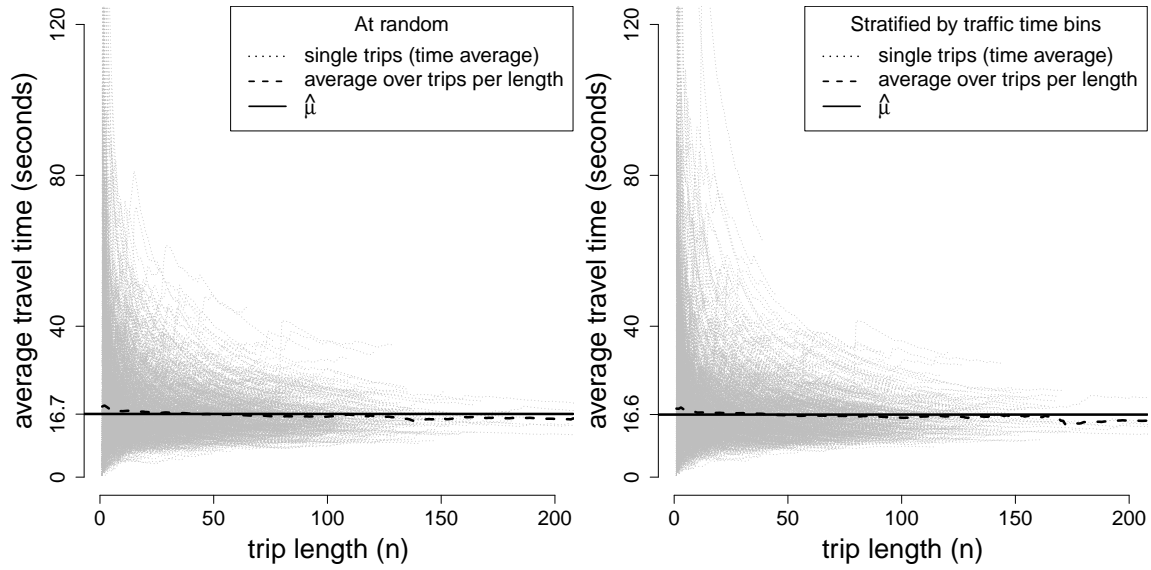


Figure S5: Time and space averaging for 1,000 trips sampled at random (left), and for the 1,500 trips stratified by traffic-bins (overall estimation, right). All trips are of at least 10 edges. Time average of each trip is in gray, dashed lines represent (space) averaging over trips per length, and solid lines are the estimates  $\hat{\mu}$ .

Table S5: Parameter estimation under different sampling methods. The "overall" estimate represents the average of the estimate per bin.

	Sampling method				
	At random		Stratified by traffic-bins		
	overall		AM	PM	Non-rush
$\hat{\mu}$	16.70 (16.4,17.1)	16.60 (16.2,16.9)	17.90	17.70	13.70
$\hat{\mathbb{V}}(n^{-1}\mathcal{T}_\rho)$	33.50	34.10	52.90	33.40	23.00
$\hat{\mathbb{E}}[n^{-1}]$	0.02	0.02	0.02	0.02	0.02
$\hat{\sigma}_{\text{prof}}$	41.80	42.20	52.80	39.90	33.00

Table S6: Model assessment under different sampling methods for the asymptotic method. All metrics are in seconds, if not a percentage.

	At random		Stratified sampling from traffic bins		
	Overall	AM	PM	Non-rush	
RMSE	379.94	382.10	383.43	384.48	288.10
MAE	285.09	291.34	289.79	267.79	194.26
ME	-17.56	27.29	-47.36	15.70	-6.17
MAPE (%)	26.83	24.47	26.59	26.15	23.38
Empirical cov. (%)	94.20	94.74	97.80	93.60	95.60
PI length	1388.1	1363.2	1760.2	1254.5	1022.3
PI rel. length (%)	140.5	134.2	167.9	136.6	137.1

Table S7: Model assessment for the asymptotic method for trips with different lengths (sampled at random).

	$n \leq 40$	$40 < n \leq 80$	$80 < n \leq 120$	$n > 120$
MAPE (%)	34.84	26.40	24.77	21.48
Empirical cov. (%)	95.00	95.00	94.60	96.00
PI rel. length (%)	242.63	137.51	110.23	92.21

## G.2 Numerical results

Table S6 illustrates various numerical results for the same test set used in Figure 3, and in addition to the results in table 2.

The following table illustrate coverage interval metrics in relation to trip length ( $n$ ).

Table S8 reports additional numerical results to those in Table 3 on a test set of 2000 trips (851 AM strata, 741 PM, and 408 Non-rush). The estimate  $\hat{\xi}_G$  is consistently close to 0.3 across all sampling methods.  $\hat{\nu}$  estimates for is 1.38 for PM, and 1.42 for Overall stratas (calculated as the average over AM, PM and Non-rush) strata.

Table S8: Model assessment for the trip-specific method under different sampling methods. Numerical results associated with prediction intervals are listed for  $N(0, \hat{\nu})$  and  $N(0, 1)$ , separated by a comma, all metrics are in seconds, if not a percentage.

	At random	Stratified sampling from traffic bins			
		Overall	AM	PM	Non-rush
RMSE	242.17	242.19	259.58	244.74	195.28
MAE	167.60	167.60	185.83	171.26	122.89
ME	-1.85	-1.85	8.13	2.67	-30.91
MAPE (%)	14.403	14.40	15.01	14.65	12.66
Empirical cov. (%)	94.6, 84.5	94.0, 84.2	91.8, 82.7	94.7, 84.8	92.7, 86.5
PI length	850.6, 587.3	827.2, 58.2	810.6, 616.4	855.8, 618.3	631.2, 454.4
PI rel. length (%)	81.3, 56.1	79.1, 55.8	71.4, 54.3	83.0, 60.0	71.7, 51.6

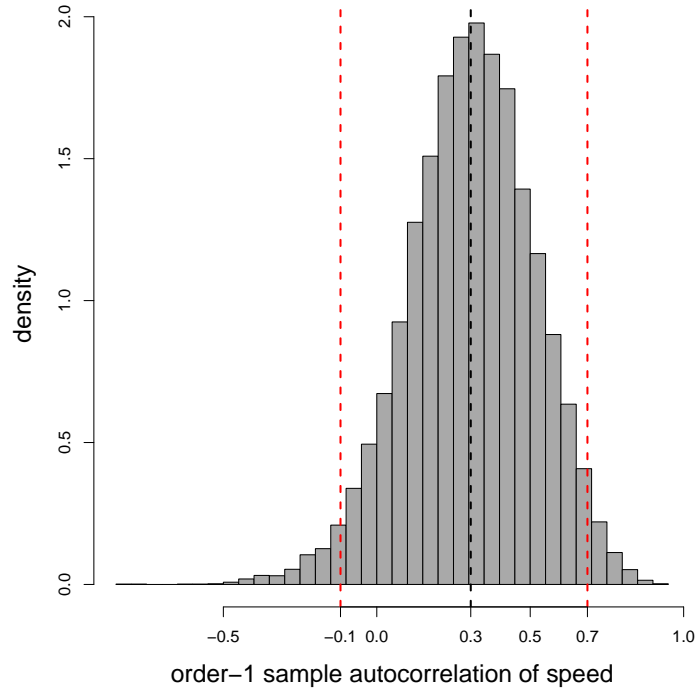


Figure S6: Histogram of  $\xi_G$  in (26) of all trips in the training of 17967 trips described in Section 6.5. The mean is indicated with black dashed lines, and the 95% empirical confidence intervals are in dashed red.

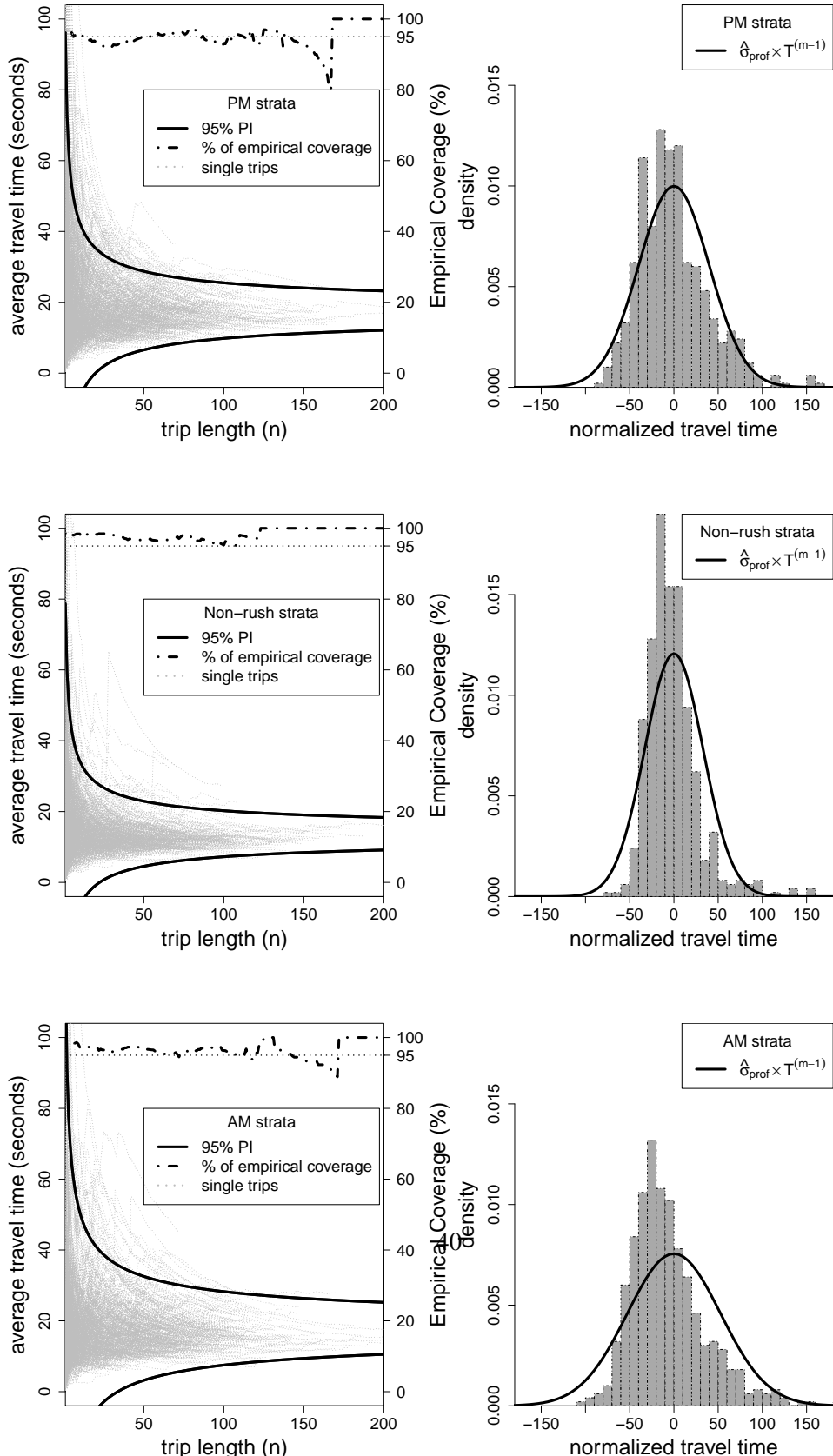


Figure S7: Average ( $n^{-1}\mathcal{T}_\rho$ ) and normalized ( $(n + nm^{-1})^{-1/2}(\mathcal{T}_\rho - n\hat{\mu})$ ) travel time for 500 test trips plotted on the left and right panels, respectively. Test trips are sampled from PM strata (top row) and from the Non-rush strata (bottom row). Prediction intervals of (20) are in solid lines. Empirical coverage levels, for each  $n$ , are in dotted lines (left panel). Right panel prediction

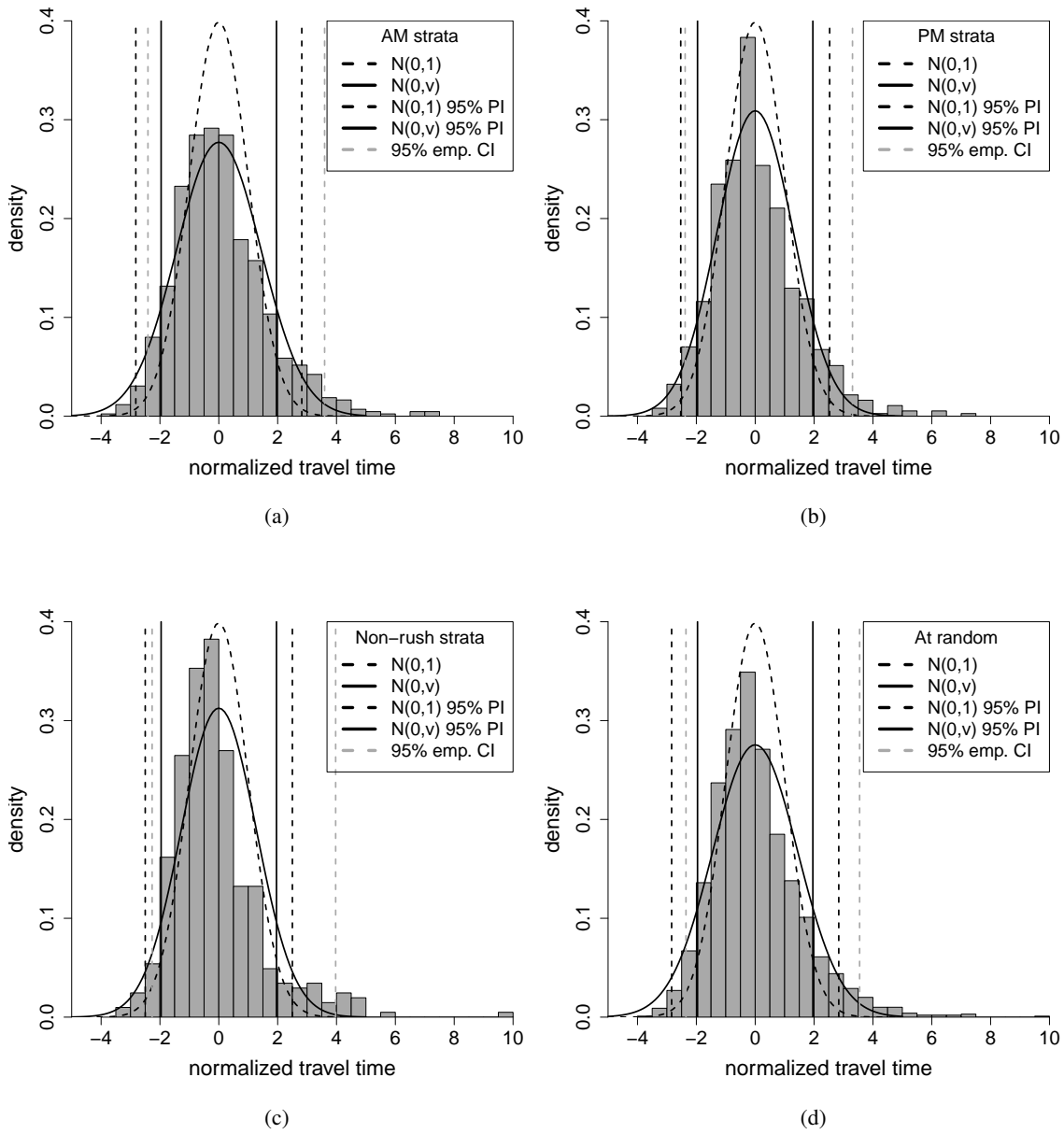


Figure S8: Histogram of normalized trips (as  $\hat{\sigma}_\rho^{-1}(t^*)(\mathcal{T}_\rho - \hat{\mu}_\rho(t^*))$ ) from the test set under different sampling methods, with a  $N(0, 1)$  density depicted in dashed black,  $N(0, \hat{v})$  in solid black; 95% prediction intervals are in vertical lines in accordance with density line; in vertical dashed gray is the 95% empirical coverage intervals.